DEVELOPMENT AND EVALUATION OF PERFORMANCE OF A BENCH SCALE GASIFIER FOR SUB-BITUMINOUS COAL

STELLAMARIS NDUKU NZOVE

MASTER OF SCIENCE
(Mechanical Engineering)

JOMO KENYATTA UNIVERSITY OF AGRICULTURE AND TECHNOLOGY

2021

Development and Evaluation of Performance of a Bench Scale Gasifier for Sub-Bituminous Coal

Stellamaris Nduku Nzove

A thesis submitted in partial fulfillment of the requirement for the degree of Master of Science in Mechanical Engineering in the Jomo Kenyatta University of Agriculture and Technology

2021

DECLARATION

This thesis is my original work and has not been presented for a degree in any other university.

Signature: ..... Date .....

Stellamaris Nduku Nzove

This thesis has been submitted for examination with our approval as the University Supervisors:

Signature: ..... Date .....

Dr. Eng. Hiram M. Ndiritu (Phd.)

JKUAT, Kenya

Signature: ..... Date .....

Dr. Benson Gathitu (Phd.)

JKUAT, Kenya

DEDICATION

I dedicate this work to my loving family. A special feeling of gratitude to my dear husband Victor, our children Adrian and Talia. They have been a great source of inspiration throughout my entire research period.

ACKNOWLEDGEMENTS

The author wishes to sincerely appreciate a number of individuals for their vital roles in the realization of this thesis. First and foremost is the Almighty God, the giver and sustainer of life, for giving me the opportunity to do this research. Special appreciation is due to Dr. Eng. Hiram Ndiritu and Dr. Benson Gathitu, my two very able and highly knowledgeable project supervisors for guiding and supporting me throughout this research. My sincere gratitude also goes to Bernard Owiti, Obadiah Maswai and John Ng'ethe, for their positive criticism which helped to keep me going. I also thank the members of staff in the department of Mechanical Engineering and Engineering workshops (JKUAT) for their assistance during the research work. Special gratitude goes to the Engineering workshops manager, Dr. P. Kihato for his invaluable counsel and encouragement during this research and also for granting the permission to use workshop equipment and facilities. During the experimental work, I got a lot of assistance from the staff in different laboratories notably Eric Waiyaki of Thermodynamics Lab, David Chitai of Welding shop, Mwai of Foundry shop (JKUAT), Johnson Mwandi among others. I am sincerely grateful to you. Finally, I extend my gratitude to my mum, brothers and sisters for the moral support that they gave me throughout the research period.

TABLE OF CONTENTS

LIST OF FIGURES

LIST OF TABLES

LIST OF APPENDICES

LIST OF ABBREVIATIONS

GHGs	Greenhouse gases
PC	Pulverized coal
IGCC	Integrated gasification combined cycle
CCTs	Clean coal technologies
CFB	Circulating fluidized bed
SCPC	Supercritical pulverized coal plant
FGD	Flue gas desulphurization
CCS	Carbon capture and storage
ESPs	Electrostatic precipitator
SCR	Selective catalytic reduction
HRSG	Heat recovery steam generator
AFT	Adiabatic Flame temperature
COE	Cost of electricity
USC	Ultra supercritical
WGS	Water gas shift
LHV	Lower Heating Value
HHV	Higher Heating Value
CGE	Cold Gas Efficiency
CCE	Carbon Conversion Efficiency
AFR	Air Fuel Ratio
TLV	Threshold Limit Value
PPM	Parts Per Million
COV	Coefficient of Conversion

SYMBOLS

English symbols

$\mathbf{g}$	Acceleration due to gravity
$\mathbf{U}_f$	Fluidization velocity
$\mathbf{T}_R$	Reactants Temperature
$\mathbf{T}_P$	Adaibatic Flame temperature
$\mathbf{T}_{aver}$	Average temperature

Greek symbols

$\boldsymbol{\phi}$	Equivalence ratio
$\boldsymbol{\rho_g}$	Density of fluidizing gas
$\boldsymbol{\rho_p}$	Density of coal particles
$\boldsymbol{\mu_g}$	Viscosity of fluidizing gas
$\boldsymbol{\dot{m}}$	Mass flow rate
$\boldsymbol{\eta}$	Efficiency
$\boldsymbol{\xi}$	Instrumental uncertainty
$\boldsymbol{\sigma}$	Experimental uncertainty
$\boldsymbol{\epsilon}$	Void fraction
$\boldsymbol{\phi_s}$	Sphericity of sphere

Subscripts

mf	minimum fluidization
ave	Average
p	coal particles
f	Fluidization
R	Reactants
P	Products
g	Fluidization gas
sy	Syngas
c	Carbon
a	Air
C	Coal
O	Oxygen
t	Terminal
F	Fuel

ABSTRACT

Trends internationally have shown that about 60% of power in developed countries of Europe, America and Asia is from coal. Combustion of coal generates huge quantities of gaseous emissions. The rules governing emissions have become more stringent and therefore, alternative techniques of coal utilization are required for clean power generation. Recent research is geared towards higher efficiency coal gasification plants as well as fuel synthesis from syngas. In this research a bench scale gasifier was designed, fabricated and its performance analyzed. The main aim of the research was to gasify sub-bituminous coal under fluidized conditions to produce a combustible gas whose composition was to be analyzed and optimum working conditions established. Air flow rate was varied and the reactor temperature and gas composition were measured at each flow rate. Results from this research showed a 13.73% reduction in CO concentration with increase in airflow rate from 1.0 to 2.5 m^3/min. CO reduction was attributed to fact that more air enhanced conversion of CO to CO_2. As the air flow rate was increased from 1.0 to 2.5 m^3/min, the HHV of the syngas was observed to decrease from 5.667 to 4.106MJ/Nm^3. This was attributed to the reduction of CO and the increase of nitrogen composition which do not add to the calorific value of the syngas. The cold gas efficiency(CGE) and carbon conversion efficiency (CCE) of the gasifier were obtained as 64.29% and 89.89% respectively. This research can be applied in power generation by channeling the syngas produced to power gas turbines and engines. The research gives insightful information that can contribute to improved design of gasification systems.

CHAPTER ONE

INTRODUCTION

1.1 Background

Coal is a black rock made of large amounts of carbon and other elements such as hydrogen, oxygen and nitrogen among others. It is considered to be formed from organic deposition of minerals. Coal is the world's most abundant and widely distributed fossil fuel. The reserves are estimated to be 990 billion tonnes which are enough for consumption in the next 150 years based on the current consumption. Over 40% of the world's energy is obtained from combustion of coal (Li & Fan, 2008). In order to be able to meet the forecasted electricity demand by 2020, power plants with 1000MW capacity have to be built every week throughout the world of which 40% will be from coal(Doerell, 1999). Declining supplies of crude oil in combination with increased environmental restrictions to reduce greenhouse gas emissions from coal-fired power plants has led to renewed interest in gasification as a clean-coal technology(Karimipour, Gerspacher, Gupta, & Spiteri, 2013). Coal will remain the most important energy source in the world owing to it's abundance, availability and also because its cost effective.

1.1.1 Coal Gasification

Coal gasification offers one of the most versatile and clean ways of converting coal into electricity, hydrogen and other valuable energy products. Gasification is one of the best methods of producing hydrogen for tomorrow's automobiles and fuel cells. It breaks down coal into its basic elemental gases namely: CO_2, CO, H_2 and CH_4 by exposing it to hot steam and air or oxygen under high temperatures and pressures. This causes the carbon molecules to break apart and create chemical reactions that results in a mixture of carbon monoxide, hydrogen and other gaseous compounds forming what is commonly referred to as syngas.

Different studies on coal gasification in fluidized beds have been undertaken. Ocampo et al. (Ocampo, Arenas, Chenjne, & Espinel, 2003) for example studied coal gasification in a pilot fluidised gasifier at atmospheric pressure and air-steam mixture. They reported gas heating values ranging between 2.8-3.0 MJ/Nm^3. Engelbrecht et al. (Engelbrecht, North, Oboirien, Everson, & Neomagus, 2011) gasified two high ash coals in a bubbling fluidized bed gasifier at atmospheric gasifier using oxygen enriched air and steam as the gasifying agent and obtained a gas of heating value ranging between 5.75-6.12 MJ/Nm^3.

1.2 Coal and the Environment

Despite many nations relying on coal for electricity generation, it is far from being a perfect fuel. Coal like other fossil fuels is formed out of carbon and when it burns, the carbon combines with oxygen to form carbon dioxide. Carbon dioxide is a colourless and a odourless gas. When released into the atmosphere it causes global warming which is responsible for change of climate globally.

Chang et al. (Chang, Zhuo, Meng, Qin, & Yao, 2016) found that 9 billion tonnes of CO_2 are emitted into the atmosphere from fuel combustion, where by more than 83% of CO_2 comes from the combustion of coal . They also found out that in 2012, about 79% of SO_2, 57% of NO_x and 44% of particulate matter (PM) came from direct combustion of coal and about 93% of SO_2, 70% of NO_x, and 67% of PM emissions came from all kinds of coal utilization (including direct combustion emission and emission from coke stoves and other industrial furnaces). These gaseous emissions not only cause greenhouse heating which is responsible for climate change but also have a negative impact on health.

Coal is a dirty fuel to burn but technology advances have greatly reduced its negative impact on the environment in the last 20 years. Scientists have come up with methods of capturing the pollutants from burning coal before they escape to the atmosphere. Today's technology can filter 99% of total particulate matter(TPM) and remove more than 95% of the acid rain pollutants in coal as well as controlling mercury (Henderson & Topper, 2005). A report by International Energy Agency(IEA) on Energy Technology Perspectives 2017 (International Energy Agency(IEA), 2017) emphasizes that decarbonised power is the backbone of clean energy transformation . The global energy sector can reach net zero CO_2 emissions by 2060 under the 2 ^oC scenario (2Ds) which focuses on limiting the average global temperature increase to 2 ^oC (Lee et al., 2016). Scientists are now exploring clean coal technologies which limit the release of carbon dioxide into the atmosphere by burning coal more efficiently. These clean coal technologies are gasification and CO_2 sequestration.

In a coal combustion plant, heat from the burning coal is used to boil water to steam which is then used to drive a steam turbine generator. In this case, only a third of the energy value of coal is actually converted into electricity and the rest is lost as waste heat. In Contrast, a coal gasification power plant gets double duty from the gases it produces. First, the coal gases are fired in a gas turbine same way as natural gas to generate electricity. Secondly the hot exhaust of the gas turbine is then used to generate steam for use in a conventional steam turbine generator. This dual source of electricity is called combined cycle and

is more efficient in converting coal into useful electricity. The fuel efficiency of a coal gasification power plant in this type of combined cycle can potentially be boosted to 50% compared to the 33-40% efficiency common at conventional coal-based boiler plants (Wong & David de Jager and Pieter van Breevoort April, 2016).

1.3 Energy Scenario in Kenya

The Kenya population was projected to 45.8 million in 2016 (Kenya National Bureau Of Statistics, 2017). The country has experienced an increase in energy demand, which can be linked to the increase in population and industrialization. One of the key indicators of economic growth and development in a country is the level and the intensity of energy use. The high cost of energy is one of the biggest obstacles to economic activity in the country. This problem has partly made Kenya lose out on foreign direct investment. Available data shows that the cost of electricity in Kenya is US$0.150 per kWh which is four times higher than that of South Africa (US$0.040) and three times more than that of China (Institute of Economic Affairs (IEA), 2015). South Africa is considered as a main regional competitor, while China as an international developed country.
In Kenya, traditional biomass and wood have dominated the energy sector providing the basic energy needs for the rural communities, urban poor and informal sector as illustrated in Figure 1.1.

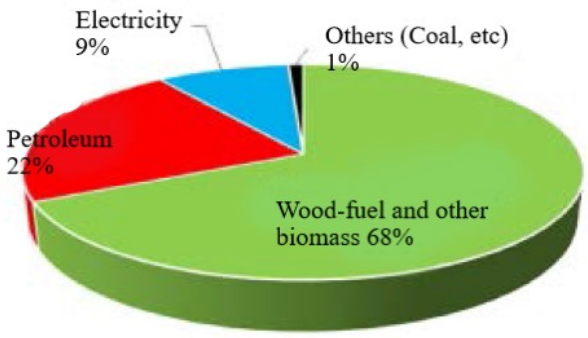

Figure 1.1: Primary Energy Supply in Kenya (Abdulganiyu et al., 2017)

A study conducted by Helio International on sub-Saharan Africa showed that dependence on wood and biomass in Kenya accounted for 68% of the total energy

consumption (Adaptation & Var, 2009). Over reliance on primary biomass energy has led to widespread exploitation of forests which are the catchment areas for Kenyan rivers. This has led to reduction in water levels in rivers and dams, which are major sources of electricity in Kenya.

Electricity in Kenya is generated from geothermal (47% of the power production), hydropower (39%), thermal (13%) and wind (0.4%). As at 2015 the installed electricity capacity was estimated to be 2.4GW, out of which 1.5GW was connected to grid and 500MW of which came online since mid-2014. Since hydro-power accounts for a large percentage of this capacity and is reliant on unpredictable weather conditions, the frequency of power outages is high at 33% (compared to an average of 1% for Mexico, China and South Africa) (Ministry of Energy Republic of Kenya, 2015). In 2013, Rural Electrification Agency(REA) announced that 90% of country's public facilities had been electrified suggesting that a large share of the population had access to the electricity grid. Despite this success, estimates of the national household electrification rate still remain at about 22% (Lee et al., 2016).

In pursuit to transform Kenya's economy, the Government had a road map in place to raise the generation capacity by at least 5000+MW from 1765MW as at June 2013 and by 6700MW in 2017. To fulfill this plan several options were being explored; which include key interest in coal, natural gas and renewable energy sources. Coal is not yet utilized in Kenya for power generation but in September 2014 the Ministry of Energy and Petroleum awarded AMU Power Company Limited (a special purpose vehicle by Gulf Energy, Centum Investment and Sichuan Electric Power Design & Consulting Company) the bid to develop a 1050MW gross output coal fired power plant in Lamu county(Amu Power Company Limited, 2016). The plant is expected to use super-critical technology.

Coal is an indigenous energy source of energy and if it is properly utilized it can help the country achieve its Vision 2030. This research is aimed at bringing the clean utility of coal as an energy source to the ordinary Kenyan.

1.4 Problem statement

The demand of electricity has been growing at an alarming rate owing to the rapid growth in population and industrialization. Peak demand increased from 899MW in 2004/05 to 1,468MW in 2013/14. The peak load was expected to increase to 2,511MW by 2015 and 15,026MW by 2030 in order to help the country achieve the projected economic growth (Ministry of Energy Republic of Kenya, 2015). This implies that the power generation capacity ought to be expanded

in order to meet these requirements. The discovery of coal in Mui basin in Kitui County is a very big boost to the country in terms of energy generation. Owing to the increasing population and need to grow the economy especially in the developing countries like Kenya, energy supply ought to be sustainable, affordable and reliable. Kenya for example is in the pursuit of achieving Vision 2030, which targets full industrialization by year 2030. To achieve this, energy has been identified as one of the key enablers to this goal. Currently the power plants in Kenya cannot meet this demand which makes the energy costs to be relatively high. This calls for other alternative sources for power generation, which are cheaper and reliable to supplement the existing supply. Renewable energy sources like wind, solar, bio-fuels among others are being explored for power generation but this is not sufficient owing to their low energy density.

With the discovery of coal in Mui basin in Kitui county, clean coal combustion for power generation has become a major area of research. Coal is one of the cheapest and oldest energy sources in the world but its combustion produces huge quantities of harmful emissions unlike other energy sources. The existing coal power plants are; pulverized coal plants (sub-critical, super-critical and ultra super-critical) and circulating fluidized bed plants. Both involve direct combustion of coal producing a lot of GHG emissions to the atmosphere. Conventional coal power plants have low efficiencies in power generation. For these plants, post combustion capture is utilized for flue gas clean up but the method is very expensive. In order to keep the environment clean there is need to utilize clean coal alternative for power generation. Integrated gasification combined cycle (IGCC) plants have proved to be one of the viable methods of utilizing coal cleanly owing to their almost zero emission advantage(Q. Liu, Shi, & Jiang, 2009). The IGCC process is not yet fully developed as compared to other methods of coal utilization (Campbell, McMullan, & Williams, 2000).There is no much information and data available on the optimum condition of performance of the coal gasifier, which is a major component of the IGCC plant. Optimization of the gasifier will improve the quality of syngas produced which will in turn improve the efficiency and cost of these units

1.5 Objectives

The main objective of this research was to develop and optimize the performance of a coal gasifier for production of syngas that can be utilized for power generation. The above main objective was to be achieved via the following specific objectives:

1. To design and construct a bench scale coal gasifier.

2. To evaluate performance of the gasifier under the influence of various flow conditions (temperature and air/coal flow rate).

3. To analyze the syngas obtained from the gasifier.

1.6 Justification

With the increasing population and the need to expand industrialization, energy demand is on the increase and the country is faced with the challenge of expanding power generation. Options for power generation currently being explored include; nuclear power, renewable energy sources and coal power plants. The net energy ratio of coal is as high as 80 compared to nuclear power, wind energy and photovoltaic cells that have moderate net energy ratios (Jonathan M. Harris, 2017). Renewable energy sources like solar and wind are encouraging but the energy density (energy per unit volume or energy per unit mass) is low and the supply is intermittent compared to fossil fuels like coal and petroleum products (Layton, 2008). For example, by 2014 the generating capacity of renewable energy in Europe was about 216 GW, 22% of Europe's capacity but the actual output was only 3.8% of Europe's requirement (Lyman, 2016). An analysis on economics of renewable energy in Tanzania by Baraka *et. al* (Kichonge, Mkilaha, & John, 2016) revealed higher primary energy supply tied with less investment costs on business as usual scenerio (from hydros, coal, natural gas, thermal power plants) compared to renewable energy scenerio. Nuclear systems have high power density but the cost of installation and maintenance are very high compared to other energy sources. In addition, following the Fukushima crisis in March 2011 many nations announced withdrawal from nuclear power. For example, in 2008 Energy Information Administration in the United states projected almost 17 Gigawatts of new nuclear power reactors by 2030, but following the Fukushima Daiichi disaster its projections by 2030 scaled back to just 5 GW (Jorant, 2011).The current exploration by the Ministry of Energy in Kitui County has shown that there are huge local coal deposits that are suitable for increasing power generation. Nations like the United States, Poland, South Africa and China have coal as their major energy source and that explains their level of economy. For Kenya's economy to grow, it is the high time the country utilized coal in power generation owing to its low cost. Clean coal technologies should be emphasized to safeguard the environment and IGCC plants are more suited as they utilize coal cleanly and have the capacity of achieving high efficiencies.

1.7 Outline of Thesis

This thesis has five chapters. The current chapter is introduction to the research which presents a general overview of the existing problem related to coal use in power generation. Chapter two presents the literature review where conventional methods of utilizing coal are highlighted. The experimental set up and the measured parameters to optimize the performance of a bench scale gasifier are outlined in chapter 3. Results of composition of syngas, gasification temperatures and fluidization velocity are discussed in Chapter 4. Chapter 5 has conclusions derived from the performance testing of the gasifier.

CHAPTER TWO
LITERATURE REVIEW

2.1 Overview

Coal utilization in energy production is facing a lot of opposition owing to the fact that coal combustion releases a lot of CO_2 emissions leading to global warming effect. Sulfur and nitrogen oxides are other undesirable gases from coal combustion as they bring about acid rain. Researchers have now concentrated their efforts on clean ways of utilizing coal in power generation and this research looks at gasification.

This chapter reviews conventional ways of utilizing coal and their shortcomings, gasification technology and some of the studies that have been undertaken on coal gasification.

2.2 Gasification Mechanism

Coal gasification is an old technology that dates back to the 19th century and was used commercially to produce the so called "Town Gas" for industrial and residential lighting in Europe and America (Gregory, Furimsky, & Mourits, 2006). Discovery of electricity and natural gas paused gasification technology(Breault, 2010). The technology resurfaced again during World War II and it was used to convert coal into transportation fuels via the Fischer-Tropsch process.

Gasification is a thermo-chemical conversion process by which coal or biomass is partially oxidized to produce a combustible gas or synthetic gas also known as syngas. Syngas comprises of hydrogen (H_2), carbon monoxide (CO), carbon dioxide (CO_2), and methane (CH_4) and their proportions are determined by the gasifying agent such as air, oxygen, steam or mixture (Couto, Rouboa, Silva, Monteiro, & Bouziane, 2013).

Gasification takes place in sub-stoichiometric conditions with controlled oxygen supply. Generally 20 to 35% of the theoretical oxygen is required for complete combustion of coal at temperatures of 700^oC and above (Mamoru Kaiho and Osamu Yamadablished (National Institute of Advanced Industrial Science and Technology Japan), n.d.). The process occurs in such a manner that as coal is consumed in the gasifier, heat and new gaseous fuel is produced(Nowak, 2003). Syngas (producer gas) finds application in gas turbines or engines coupled to a generator to produce electric power. Syngas is also used in a boiler to produce heat or as a raw material for synthesis of chemicals, liquid fuels or hydrogen. Gasification takes place in a reactor called gasifier, which has provisions for feeding the fuel and gasifying agent.

The process of gasification starts by drying coal since it contains moisture which can only be removed as steam when the fuel is heated to the saturation temperature of the gasifier operating pressure. What follows is pyrolysis process. During this process light volatile gases such as hydrogen are evolved in addition to other gases, tars and phenols. The resulting char obtained from pyrolysis reacts with the gaseous reactants (oxygen, steam, carbon dioxide and hydrogen) to release gases (CO, H_2, CO_2, CH_4), tar vapors and a solid residue (char and ash)(Couto et al., 2013).

Complete gasification is governed by the following series of chemical reactions (Inc., Princeton Energy Resources International, , , & Consulting, 2003).

$$C + O_2 \rightarrow CO_2 \qquad -394\,MJ/kmol \tag{2.1}$$

$$C + \frac{1}{2}O_2 \rightarrow CO \qquad -111\,MJ/kmol \tag{2.2}$$

$$H_2 + \frac{1}{2}O_2 \rightarrow H_2O \qquad -242\,MJ/kmol \tag{2.3}$$

$$C + H_2O \rightarrow CO + H_2 \tag{2.4}$$

$$C + 2H_2O \rightarrow CO_2 + 2H_2 \tag{2.5}$$

$$C + CO_2 \rightarrow 2CO \tag{2.6}$$

$$C + 2H_2 \rightarrow CH_4 \tag{2.7}$$

$$CO + H_2O \rightarrow H_2 + CO_2 \tag{2.8}$$

$$CO + 3H_2 \rightarrow CH_4 + H_2O \tag{2.9}$$

$$C + H_2O \rightarrow \frac{1}{2}CH_4 + \frac{1}{2}CO_2 \tag{2.10}$$

Most of the oxygen or air injected in the gasifier is consumed in reactions shown by Equations 2.1 - 2.3 to provide the heat necessary to dry the solid fuel, break up chemical bonds and raise the reactor temperature to drive gasification reactions from Equation 2.4 to Equation 2.9. Reactions shown by Equations 2.4 and 2.5 are the principal gasification reactions and are endothermic requiring high temperature and low pressures. Reaction 2.6 is called *boudourd reaction* which is endothermic and much slower than the combustion reaction 2.1 at the same temperature in absence of a catalyst. Reaction 2.7 is called hydro-gasification and is very slow except at high pressures.

Equation 2.8 represents the water gas shift (WGS) reaction and it is important when hydrogen production is desired. Production of hydrogen from coal gasi-

fication became popular during the oil crisis in the late 1970s (Ayodele, Offor, Akhabue, Akhihiero, & Cheng, 2017). The reaction takes place at low temperatures of up to 260^{o}C in presence of a catalyst and is independent of pressure. Over the years Cu-ZnO has been used as the catalyst for WGS reaction though it is not attractive as it is very sensitive to temperature excursions, pyrophoric if exposed to air and requires very careful pre-activation (Fu, Deng, Saltsburg, & Flytzani-stephanopoulos, 2005). Literature review by Andreeva *et al.* (Andreeva et al., 2002) revealed Ceria-supported precious metals(Pd,Pt,Rh,) as effective catalysts for CO oxidation and WGS reaction. In their research, they used Ceria-Au catalysts for WGS reaction which demonstrated a high and stable activity over a wide range of temperatures. Ceria-precious metals catalysts are desirable as they are non-pyrophoric and can be used without activation.

Methanation reaction represented by equation 2.9 proceeds at low temperatures in absence of a catalyst. Reaction 2.10 is relatively thermal neutral meaning that gasification can proceed with little heat input but methane formation is slow relative to reactions 2.4 and 2.5 unless catalyzed by mostly Ni-based catalysts.

The syngas produced from gasification process has different chemical composition, heating value and hence different end use applications. These differences are brought about by the type of gasification agent used (air, oxygen and steam), gasifier operating pressure and temperature, the coal rank and composition, the heating rate, coal preparation and particle size and lastly the plant configuration. The plant configuration refers to coal feeding system (dry or slurry), the coal reactant flow geometry, mineral removal system (dry or slag) and syngas cleanup system.

2.3 Coal Utilization Techniques

In the past, coal has been utilized in a number of ways to produce power. These are discussed below.

2.3.1 Pulverized coal power plants

Pulverized coal power plants are among the oldest utilization methods of coal in power generation. They use rankine cycle principle and consist of a pulverized coal (PC) fired boiler, a steam turbine, pumps, Flue Gas Desulphurization (FGD) unit, generator and other auxiliaries as shown in Figure 2.1.

Finely ground coal is fed into the boiler (heat generation unit) where it is mixed with air entering from forced draft fans and combustion takes place changing its

chemical energy into heat. This heat is transferred to water running through the tubes in the boiler walls to produce steam. The steam is then passed through the super-heater where its pressure and temperature are increased before it's channeled through a series of steam turbines to generate mechanical energy. The low energy steam exhausted from the high pressure turbine is passed through the reheater for further heating before it is introduced to the intermediate and low pressure turbines respectively. The mechanical energy gained by the turbines is used to drive the rotor of the generator with a constant speed which is the synchronous speed from the rotor's mechanical rotation and the coupling magnetic field from the exciter. Voltage is then induced in the windings of the stator by Faraday's law. The steam exiting from Low pressure turbine is passed through the cooling towers where it is condensed to water and pumped to the deaerator and then to the boiler to begin the cycle again. The spent fuel ends up in the ash hopper and the exhaust gases are discharged through the stack.

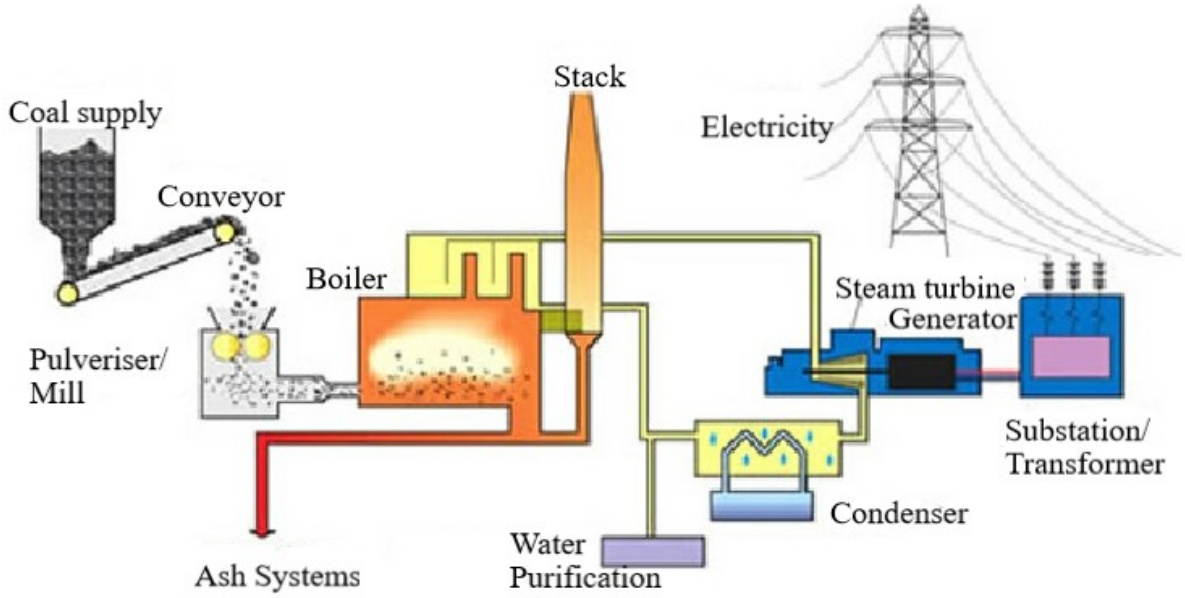

Figure 2.1: Schematic diagram of a Pulverized Coal Power Plant (Staff & Project, 2006)

Pulverized coal power plants produce substantial amounts of emissions like sulphur dioxide(SO_2) and nitrogen oxides (NO_X) that are major causes of acidic rain. Particulate emissions are also common from such power systems that cause formation of smog.

The plants use post combustion processes for cleanup of the flue gases which increase the capital cost of the plant. For example, fitting a carbon capture system

requires additional power. This is compounded by the fact that the concentration of carbon dioxide in the flue gases is low at about 13% (H. Liu, Ni, Li, & Ma, 2008). In addition, the carbon capture units reduce the efficiency of the plant by about 9-13% because of their high energy consumption rate.

Calin *et al.* (Calin-Cristian Cormos & Babes, 2012) estimated and compared the key techno-economic and environmental performance indicators of PC plants (both subcritical and supercritical cases) and integrated gasification combined cycle (IGCC) case with and without CCS (carbon capture and storage unit) using CAPE tools. They found out that introducing CCS unit had an energy penalty to the PC plants (8-9%) while IGCC energy penalty was about 7%. The cost implication for fitting CCS in PC plants was much higher than in IGCC case . A conceptual layout of a PC plant having a CCS units is shown in Figure 2.2.

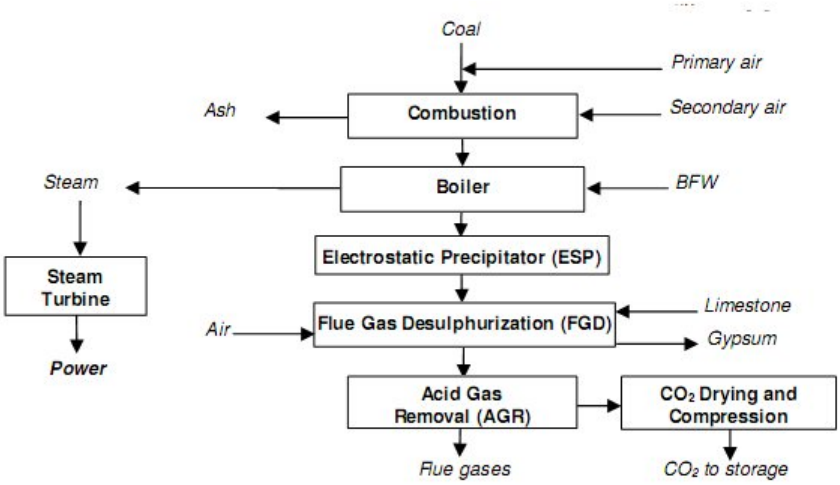

Figure 2.2: Conceptual layout of PC plant for power generation with CCS (Calin-Cristian Cormos & Babes, 2012)

2.3.2 Supercritical pulverized coal power plants

Supercritical pulverized coal (SCPC) plants are a modification of pulverized coal power plants that generate steam at a high temperature and pressure. This makes them to have higher efficiency than PC plants. Emission of pollutants in SCPC plants is lower compared to PC plants since less coal is used. They face same challenges of post-combustion clean up as PC plants.

Bohm *et al.* (Bohm, Herzog, Parsons, & Sekar, 2007) explored options which could be taken into consideration during the the initial design and construction of PC and IGCC plants to reduce capital costs and energy losses associated with

retrofitting for CO_2 capture. Three scenarios were considered namely baseline supercritical PC, baseline IGCC and an IGCC plant with pre-investment for capture. They found out that the baseline supercritical PC plants are more preferred than the baseline IGCC and IGCC with pre-investment plant for a case where there is no carbon price. With introduction of higher carbon prices, baseline IGCC and IGCC with pre-investment plants become the most economical.

2.3.3 Circulating fluidized bed(CFB)

In CFB plants, crushed coal and limestone or dolomite (used for SO_2 capture) are fed into a bed of ash and coal particles. Using high velocity preheated air, the materials are then made highly mobile. To control NO_X formation, air is fed in the combustion chamber in two levels. The combustion chamber is a shell tube heat exchanger i.e as water travels through tubes on the walls of the chamber it is heated producing steam. The combustion products travel through the combustor and on to a cyclone where the solids are separated from the flue gases and sent back to the combustor for further oxidation. The hot flue gases are then passed through heat exchangers to produce more steam to drive the steam turbine coupled to a generator to produce electricity (Professor Prabir Basu, 2006). The process is illustrated in Figure 2.3.
Nowak *et al.* (Nowak, 2003) studied CFBs installed in Poland based on boiler design parameters, design arrangement and specific design features. He found out that the boiler designs could allow combustion of a variety of fuels ranging from high sulphur coal, lignite, peat, oil, sludge, petroleum coke among others. The CFBs installed were able to meet the minimum levels for SO_2 and NO_X emissions required but the systems did not have carbon capture units. This means the CFBs have high level of carbon emission that is responsible for global warming.

2.4 Fluidization Phenomena

Fluidization is the process by which fine bed of solids are transformed into a fluid like state through contact with a gas or a liquid. Bubbles are usually formed within the bed which then move upwards towards the combustors disengaging height. The bubbles carry a portion of the bed material along with them in a portion called wake and on reaching the maximum disengaging height the bubble bursts through the surface and the portion of bed material falls downward in the reactor by gravity. The free falling particles are balanced by the upward force of the minimum fluidization velocity of bed materials. New bubbles are formed

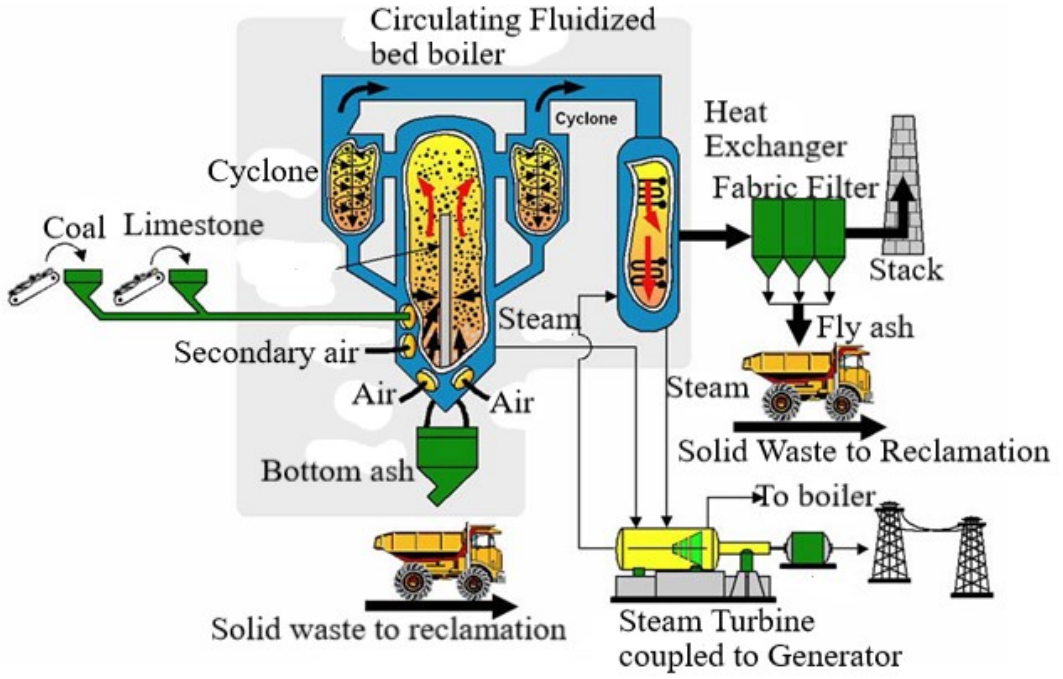

Figure 2.3: Diagram of a Circulating Fluidized Bed Combustor (Reclamation, n.d.)

and the cycle is repeated. This process promotes proper mixing of the fuel and the oxidizing agent and good heat distribution allowing for uniform temperature within the reactor(Dayananda & Sreepathi, 2012). Depending on the fluidization velocity the fluidized beds are classified as packed, bubbling or circulating or turbulent(Professor Prabir Basu, 2006). A diagram of a fluidized bed gasifier is illustrated in Figure 2.4.

2.4.1 Mass of solid in the fluidized bed

There is a drag force exerted on the bed particles by the flowing air and at low velocities the pressure drop relating to this drag follows Ergun equation (Suleiman et al., 2013). By increasing the velocity a point is reached when the total drag on the particles will equal the weight of the bed and the particles will begin to lift and barely fluidize as shown in Equation (2.11)

$$W_s = \rho_s A_s h(1 - \varepsilon) \tag{2.11}$$

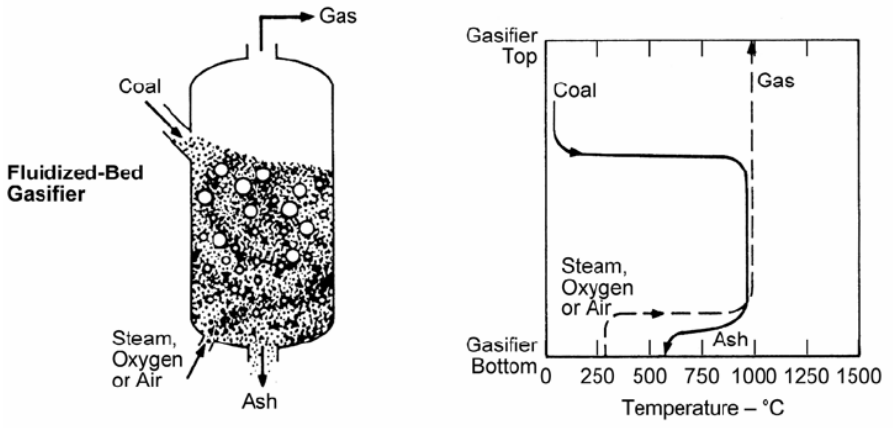

Figure 2.4: Diagram of a Fluidized Bed Gasifier (Phillips, 2006)

where W_s is the mass of solids in the bed, ρ_s is the density of the solid, A_s is the cross−sectional area of solid, h is the height of the bed settled before the particles start to lift and ε is the void fraction of the bed. The void fraction is expressed as shown in Equation (2.12)

$$\varepsilon = 1 - \frac{m_s}{\rho_s \times v_s} \tag{2.12}$$

where m_s is the mass of the particles and v_s is the total volume occupied by the bed of particles.

The observable parameters in a fluidized bed are the pressure drop (ΔP) needed across the gasifier to cause the fluid to flow the bed of particles , the fluid velocity (u) and the density of solids (ρ_s). The Ergun equation relates all these parameters as shown in Equation (3.6)

The bed expansion as the fluidization velocity is increased is illustrated in Figure 2.5 If the gas velocity is increased such that the drag on an individual particle surpasses the gravitational force on the particle then the particle is entrained in the gas and carried away from the bed. This condition is called elutriation. The velocity at this point is called elutriation velocity. The minimum elutriation velocity for particles of a given size is the velocity at incipient entrainment and is assumed to be equal to the terminal velocity (u_t).

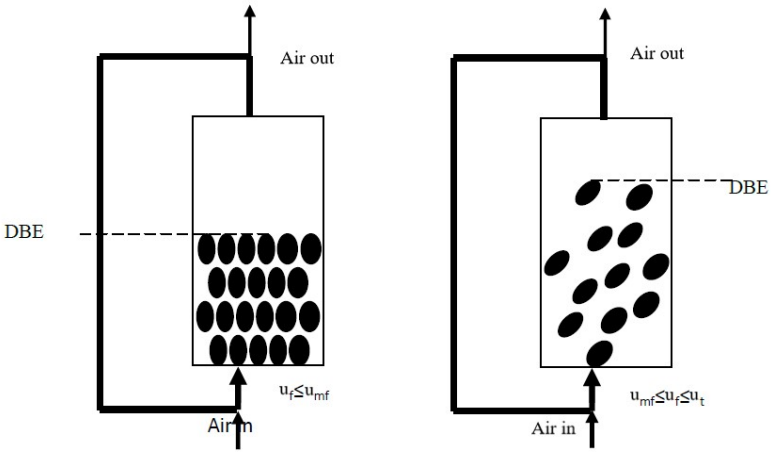

Figure 2.5: Conceptual fluidized reactor containing uniform particles with degree of bed expansion (DBE) as related to fluidization velocity u_f (Suleiman et al., 2013).

2.5 Integrated gasification combined cycle (IGCC)

2.5.1 Background

Integrated gasification combined cycle (IGCC) power plant combines two technologies in its operations; coal gasification and the combined cycle for electricity generation. Combined cycle consists of gas turbine/generator, a heat recovery steam generator (HRSG) and a steam turbine/generator. The process starts by feeding a carbon containing material to the gasifier along with oxygen and steam to produce syngas. The syngas produced passes through a series of cleaning processes to remove particulate matter and sulfur. Pre-combustion clean up makes NO_X and SO_2 controls to be less expensive as compared to post combustion controls. The clean syngas is then combusted in the gas turbine coupled to the generator to produce electricity and the heat from the exhaust is recovered in the HRSG to produce steam. The steam is then expanded through a steam turbine to power another generator to produce more electricity. The process is more efficient than other conventional power generating plants because it re-uses waste heat to produce electricity. This process is illustrated in Figure 2.6.

For IGCC plants fitted with Pre-combustion Capture units, the syngas is passed through a shift reactor and an absorption tower to remove carbon in form of CO_2 as shown in Figure 2.7. The shift reactor reacts CO in the syngas with water to form H_2 and CO_2 with the latter going to sequestration.

Emissions are easily controlled in IGCC plants because the syngas produced is at high temperature and pressure and contains higher concentration of pollutants

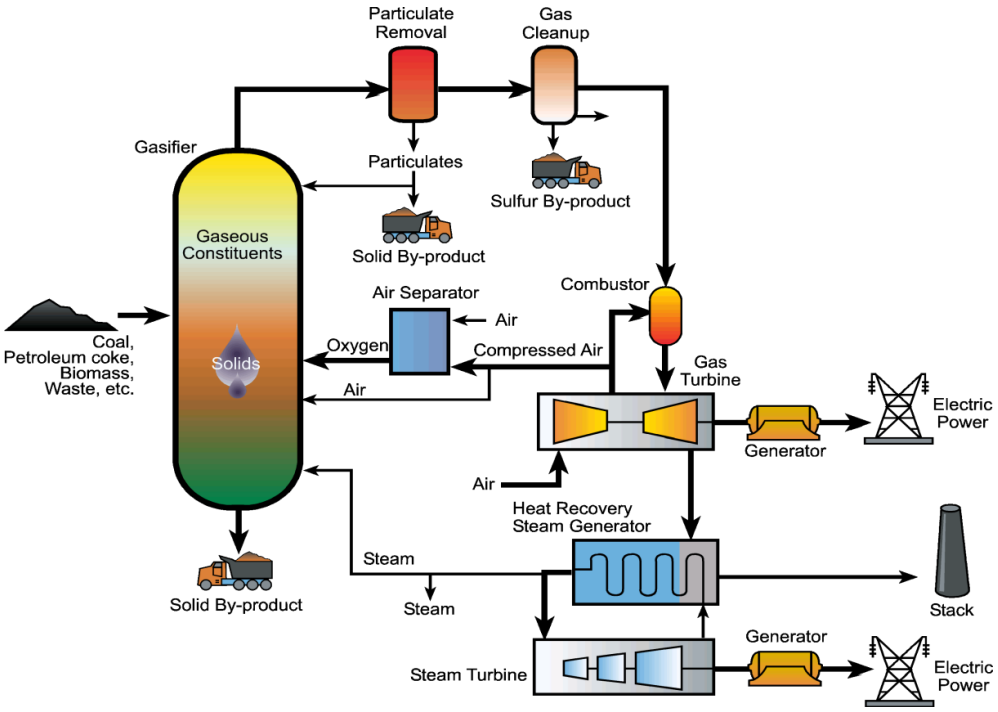

Figure 2.6: Layout of IGCC power generation scheme without carbon capture (Breault, 2010)

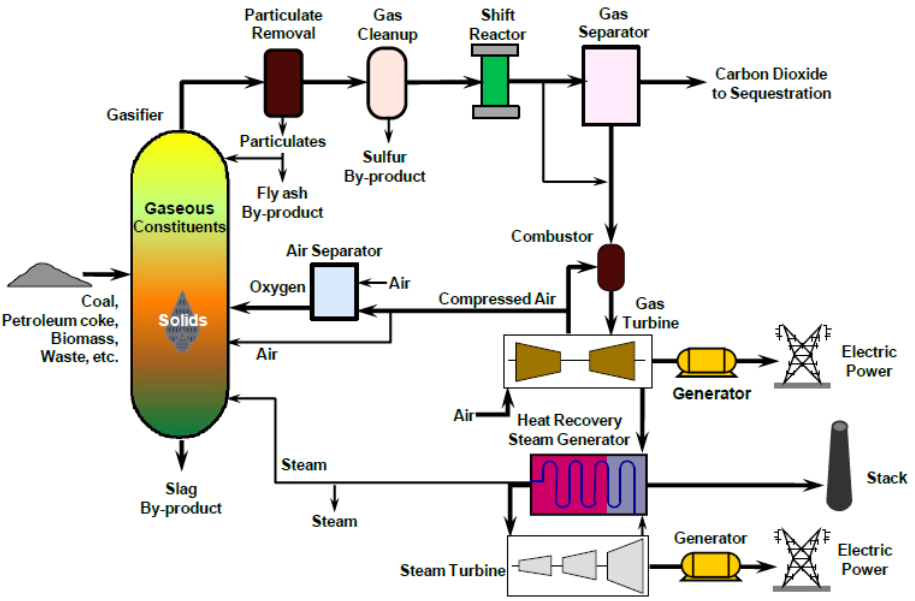

Figure 2.7: Layout of IGCC power generation scheme with carbon capture (Breault, 2010)

than exhaust gas from traditional coal-fired power plants making the cost of removal of pollutants cheaper (Martelli, Kreutz, & Consonni, 2009). For pollutants such as NO_x SO_2, particulate matter and Hg, IGCC is inherently lower polluting

(about 1/10) than traditional coal fired fire plants. The desulfurization rate is 99% while the denitrification rate is 90% and nitrogen oxide emissions are 15-20% of that of conventional power plants (Henderson & Topper, 2005).

Integrated gasification combined cycle plants are also very flexible as far as feedstock is concerned, for example various grades of coal can be accommodated in addition to wastes, biomass, petroleum coke and other refinery products. The syngas after cleaning can be used for production of electricity, chemicals, liquid fuels(methanol, dimethyl ether(DME)). Other products from IGCC plants are hydrogen, synthetic natural gas, a range of fertilizers and glassy slag that can be used as a material for cement and road surfaces (Shadle, Breault, & Bennet, 2017).

The IGCC plants have relatively high efficiencies than other coal power plants. This is mainly due to the decreased energy requirement in removal of CO_2 from the process streams in gasification as compared to PC plants. Moreover, IGCC plants use less cooling water and are desirable if the plant is to be put up in dry areas. The IGCC power plants though highly competitive are relatively expensive and have low availability. Henwei *et al.* (H. Liu et al., 2008) studied the reasons why China needed to deploy IGCC technology and the rational driving force to develop IGCC in China. This was done by reviewing several advances in IGCC technology in countries like USA, Japan, Germany and Holland. The driving forces for deploying IGCC power technologies in China like the other countries had done were found out to be the ability to satisfy electricity demand, almost zero emission technology and to aid in oil shortage problems.

Lifeng *et al.* (Zhao, Xiao, Sims, Wang, & Xu, 2008) evaluated the technical, environmental and economic dimensions of deploying advanced coal fired power technologies in China. They tried to estimate the capital cost and the overall cost of electricity (COE) for a variety of advanced coal power technologies based on technological and economic levels in 2006 in China. The options considered were nine PC cases, three subcritical (SC) and three USC (ultra supercritical) all with or without pollution control equipment; one CFB case and two IGCC cases utilizing multi nozzle coal-slury entrained flow gasifier, and shell gasifier. They found that the design efficiency for IGCC plants was almost equal to SC case and little lower than USC case. IGCC case was found to have the best environmental performance compared to other PC plants. Capital costs and COE were very high for IGCC case compared to other cases. Compared to other cases IGCC technology was in testing and demonstration stage that could explain the high costs. They only used one type coal in there study(shendong coal) probably using

a variety would have given different results.

2.6 Parameters Influencing Performance of Gasifiers

The success of gasification process is greatly affected by the working parameters which include pressure, temperature, residence time, gasifying agent, particle size. Depending on the gasifier system configuration, operating conditions and the gasifying agent, the syngas produced can be of low heating value (3.8-7.6MJ/m^3), medium heating value (10.5-16MJ/m^3) or higher heating value gas (over 21MJ/m^3). Below are some of the studies by researchers on how these parameters affect the syngas output.

2.6.1 Influence of Pressure and Temperature

Alexander *et al.* (Tremel, Haselsteiner, Kunze, & Spliethoff, 2012) studied the gasification kinetics of Rhenish lignite, bituminous coal and German anthracite in a pressurized high temperature entrained flow reactor (PiTER). This was done at high temperatures (1800^oC), high pressure (5MPa) and within a reducing gas environment. The experiments were carried out in pilot scale and bench scale. PiTER is specifically designed for experiments and enables measurements over a wide range of operating conditions. The conversion rate was found out to be directly proportional to the pressure and residence time for all samples of coal with lignite showing better response owing to its high reactivity. The gasification rate increases exponentially with temperature. Thermal annealing limits mass transfer which reduces char reactivity at temperatures between 1400 to 1600 ^oC. Therefore, it is necessary to establish a mechanism of overcoming this limitation.
Feng *et al.* (Feng Duan, Lihui Zhang, 2011) studied the effect of pressure on coal gasification characteristics by using a pressurized turbulent circulating bed. They found that the product quality was improved at higher pressure because of the better fluidization in the reactor. HHV increased by 17% and carbon conversion increased from 57% to 77% when pressure was increased from 0.1 to 0.3 MPa. Their research used high ash fusion coal and the relationship between low ash fusion coal and pressure was not shown.
Hao *et al.* (H. Liu et al., 2011) studied the effect of heating rate during pyrolysis on the gasification reactivity of three types of char in CO_2 at elevated temperatures in a novel fluidized bed. They found out that higher heating rate during pyrolysis led to higher char reactivity of gasification and was more pronounced for char derived from coal with high volatile content. Air was used during pyrolysis

and the CO_2 was mixed with N_2 which would result to high production of NO_X emissions owing to the high temperatures involved.

2.6.2 Influence of Gasifying agent(oxygen, air, steam and oxy-fuel (O_2/CO_2))

Umeki *et al.* (Umeki, Yamamoto, Namioka, & Yoshikawa, 2010) conducted a high temperature steam only gasification experiment by applying steam with temperatures exceeding 1200K in a demonstration plant with coal rate of 1.2 ton/day. They also used numerical analysis to analyze the results. They found that the steam/carbon ratio had a significant effect on the gas compositions through the water gas shift reaction . The major draw back of this research was the low reaction rate which was caused by the gas shift reaction which is endothermic thus external heating was necessary to sustain the reactions.

Several other studies done in the past in an effort to improve gasification include; study done by Na *et al.* (Na, Park, Kim, Lee, & Kim, 2003) that showed that the composition of H_2 and CO was dependent on oxygen/fuel ratio in an oxygen blown gasification process. They did so by gasifying combustible waste mixed with plastic and cellulase materials in a fixed bed gasifier using oxygen as the gasifying agent. The research failed to capture on emissions from the process which is key if the process is to be put into practice.

A numerical study done by Chen *et al.* (C. Chen, Horio, & Kojima, 2000) in their effort to show the effects of operating conditions on gasifier performance, revealed that the air to coal ratio had pronounced influence on the heating value of the product gas in a two stage-air blown gasifier.

Choi *et al.* (Choi, Li, Park, Kim, & Lee, 2001) studied coal gasification characteristics in an entrained flow gasifier. They did so by constructing a comprehensive numerical model to simulate the coal gasification process which was divided into several simplified stages such as slurry evaporation, coal devolatization and two phase reactions coupled with turbulent flow and phase heat transfer. They observed that increasing the oxygen/carbon ratio caused an increase in the syngas yield of the coal gasification.

Le Wu *et al.* (Le Wu, Yu Qiao, 2012)studied ignition characteristics of Datong bituminous coal in O_2/N_2 and O_2/CO_2 atmospheres with different conditions (including O_2 and coal concentrations and temperature). They used simulation of an unsteady model of a pulverized coal cloud including sub-models of radiation and convection. They also tested ignition temperature in a small furnace. The results showed that ignition temperature decreases with increase of oxygen con-

centration with more pronounced response in O_2/CO_2 atmosphere. The ignition temperature also reduced when the atmosphere changed from O_2/N_2 to O_2/CO_2 owing to the high heat capacity and low diffusivity of CO_2. Increasing concentration to 30% O_2 60% CO_2 was found to have same ignition characteristics as in O_2/N_2. In their study they did not demonstrate how different types of coal would affect the ignition characteristics.

2.6.3 Influence of Feedstock(coal type)

Co-gasification of biomass and coal can be considered as a potential fuel-base for gasification, syngas production and methanol synthesis. Tomasz *et al.* (Chmielniak & Sciazko, 2003) evaluated the feasibility of deploying co-gasification of biomass and coal in methanol synthesis. They found it a better way of utilizing to full capacity the syngas produced, for example in cases of low electricity demand the syngas is channeled to methanol production.

Nor F. O. *et al.* (Nor Fadzilah Othman, Mohd Hariffin Bosrooh, 2007) studied how producer gas composition varied with partial gasification of different types of coal and different gasifying agents (air, air/steam). They found out that the ratio of CO and H_2 in the syngas produced changed with coal type and gasifying agent with more CO produced in the case of air. In their research they were unable to obtain airfuel ratio, air/steam/fuel ratio and the cold gas efficiency which are vital parameters.

Xiaojiang *et al.* (Xiaojiang W., Zhongxiao Z.,Guilin P., Nobusuke K., Shigekastu M., 2010) studied the gasification characteristics and slagging behaviour of Chinese ash fusion temperature (AFT) coal in a lab scale downflow gasifier. From the experiment, the carbon conversion rate increased with temperature increase whereas, CH_4 and other hydrocarbon gases concentration decreased with temperature increase. Gasification temperature and carbon conversion increased with increase in O_2/coal mass ratio. They obtained the optimum working temperatures to range between 1573K to 1623K with corresponding O_2/coal mass ratio of 0.93 to 1.13.

Harris *et al.* (Harris, Roberts, & Henderson, 2006) studied the effect of coal type on the key gasification parameters. They did this by varying the O:C ratio, residence time and coal type and observed the conversion levels and product gas composition under conditions relevant to those present in entrained gasification system. The results showed that increasing stoichiometry increased conversion levels with optimum stoichiometry levels ranging between 90-100%. Increasing O:C ratio increases the concentration of CO_2 at the expense of H_2 and CO. In

addition, increasing temperature decreases the concentration of CO_2 and increases the concentration of H_2.

2.7 Summary of Gaps

In reviewing past research work, a number of studies have been done on gasification phenomena and the following gaps have been identified.

- Gasification of coal is being utilized in large scale for power generation and little has been done for small domestic use.
- Conventional methods of coal utilization produce high quantities of greenhouse gases and putting up new plants is becoming a challenge all over the world as rules governing emissions insist on clean technologies.
- Research concerning the effect of varying input parameters during coal gasification on the performance of the gasifier is not satisfactory, for example very high temperatures in the gasifier encourage slagging of ashes which slows down the reactions and low temperatures will not favour water gas shift reaction which is endothermic.
- The efficiency of conventional coal powerplants range between 30-48%while that of IGCC power plants range between 42-50%. This means a lot of energy is lost and more research is needed to boost the efficiency.
- Low ranked coals such as sub-bituminous and lignite have been overlooked as most researchers are focusing on high quality bituminous coal.

CHAPTER THREE
EXPERIMENTAL DESIGN AND METHODOLOGY

3.1 Background

Emission of pollutants from conventional coal fired power plants has resulted to a need for cleaner methods of utilizing coal in power generation while at the same time safe guarding the environment. Of interest in this research is gasification technology which is a cleaner method of utilizing coal. The process takes place in an equipment called a gasifier and for optimum results the gasifier needs to be properly designed. This chapter therefore presents the design and fabrication of a fluidized bed gasifier. The gasifier was constructed with provisions for controlled feeding of air and fuel in order to optimize the gasification process. A set up to evaluate gasifier performance in terms of gasification temperatures, syngas composition and calorific value is presented thereafter.

3.2 Design Configuration of the Bench Scale Gasifier

The fluidized bed gasifier consisted of a fluidized bed portion, disengaging space or freeboard (section above the bed of particles) and a gas distributor, solids feeder, solids discharge points, instrumentation and gas supply.

3.2.1 Experimental Setup

The schematic diagram and the experimental set up of the bench scale gasifier are shown in Figure 3.1 and Figure 3.2 respectively.
From the diagrams, the gasifier comprised of the plenum, reactor and the free-board section is noticeable. A variable flow air blower connected to a delivery pipe to the base of the plenum can also be seen. Thermocouples attached to a data logger are also noticeable. At the top of the gasifier, an outlet pipe of the syngas is connected and it consists of a section for sampling the syngas and also holding the burning flame. At the top of the gasifier also a coal feeding point can be seen.

3.2.2 Coal Samples

Sub-bituminous coal was chosen as the feedstock for the gasification process. The coal was first pulverized to small particles and then sieved to the desired size of 3mm as shown in Figure 3.3. This was in accordance to Geldart's classification of powders shown in Figure 3.4(Dechsiri, 2004).

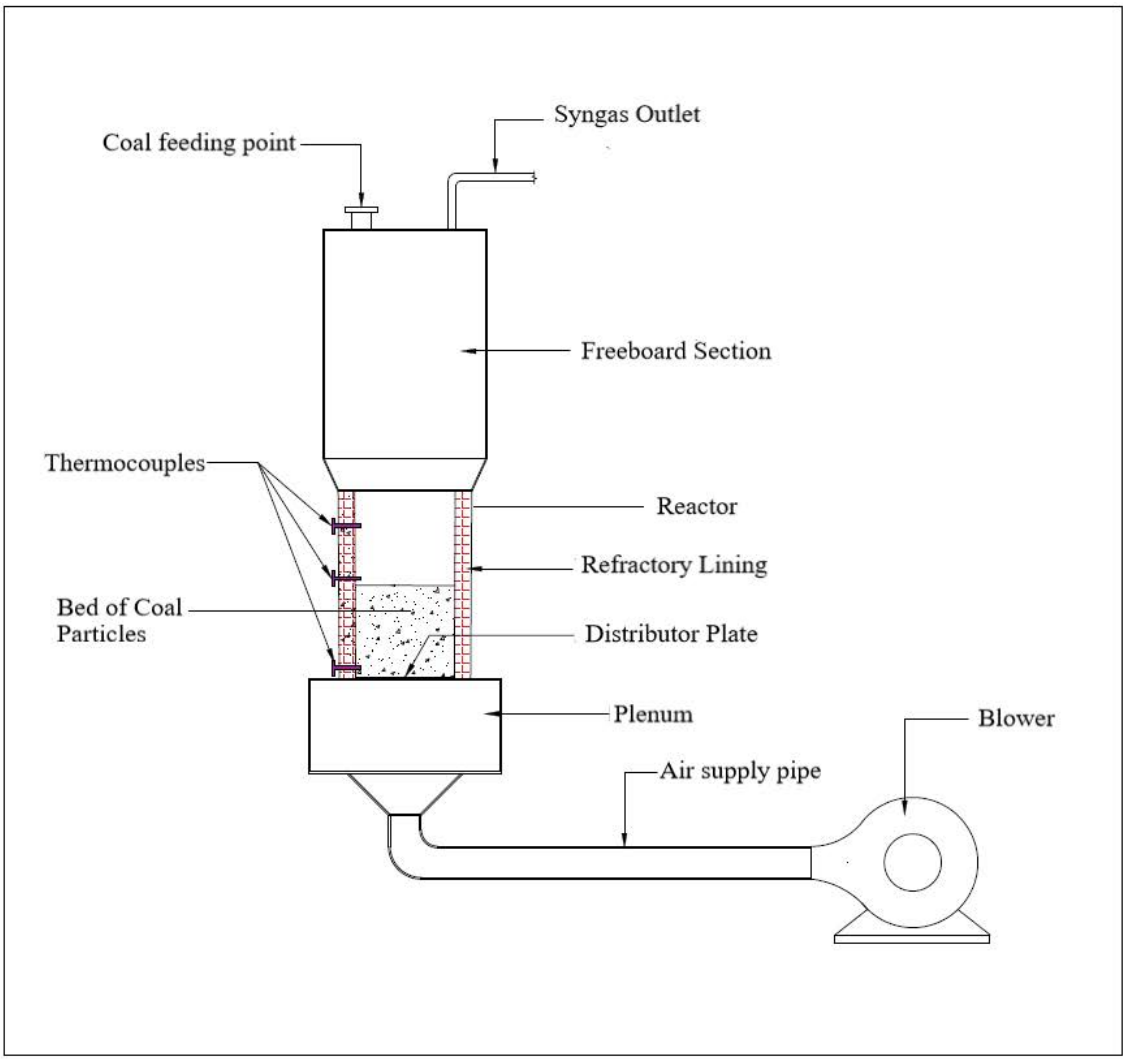

Figure 3.1: Schematic Diagram of the Bench Scale Gasifier Setup

Geldart categorized powders into four types namely group A or aerated type, group B or sand like type, group C or cohesive type and finally group D or spouted type. Group D was chosen in this research as the particle size was greater than $500\mu m$. The pulverized coal was then dried prior to use to reduce the moisture content.

3.2.3 Proximate Analysis

Proximate analysis involves determination of properties of a fuel such as the moisture content, volatile matter, ash content and fixed carbon. Moisture content was determined by drying 1g of coal sample at 105^oC (slightly above the boiling point of water) for 1 hr. The weight loss expressed as a percentage of the initial weight of the coal sample gives the moisture content as shown in Equation 3.1

Figure 3.2: Experimental Setup

Figure 3.3: Preparation of coal samples

$$\%M = \left(\frac{w_o - w_c}{w}\right) X100 \tag{3.1}$$

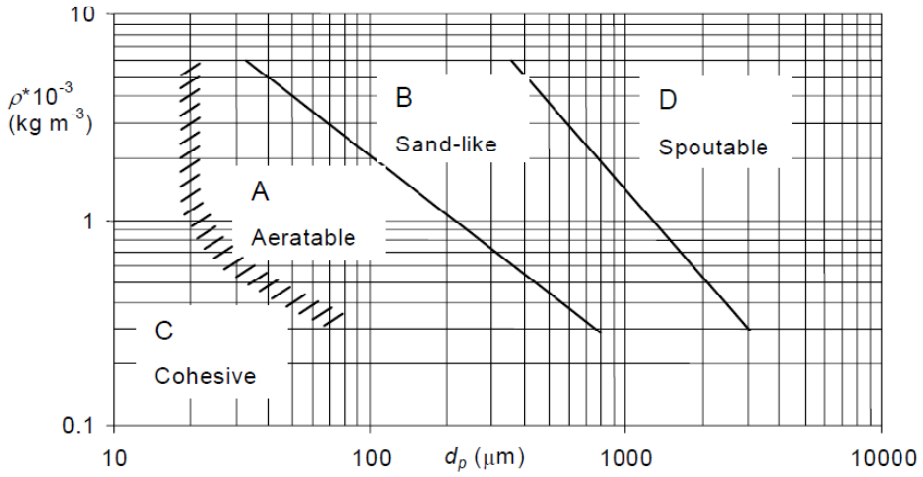

Figure 3.4: Diagram of the Geldart classification of particles (Dechsiri, 2004)

where w_o is the weight of the coal sample plus weight of the crucible, w_c is the weight of the crucible and w is the weight of the coal sample.
Ash content was determined by combustion of 1 g coal sample in a furnace at 600^oC for two hours to ensure that carbon is completely burnt. The ash content value was obtained using Equation 3.2

$$AC(\%) = \left(\frac{w_a - w_c}{w_d}\right) 100 \tag{3.2}$$

where AC is the ash content, w_a is the weight of coal sample plus weight of the crucible and w_d is the weight of the dry sample coal.
Volatile matter was obtained through combustion of 1 g coal sample at 950^oC for 7 minutes and the content was computed using Equation 3.3

$$V(\%) = \left(\frac{w_{v0} - w_v}{w}\right) 100 - \%M \tag{3.3}$$

where w_{v0} is the weight of the coal sample plus the weight of the crucible and the top, w_v is the weight of the crucible and the top plus the sample waste. Fixed carbon was obtained by subtracting the amount of moisture, volatile matter and ash content from 100%

3.2.4 Ultimate Analysis

The ultimate analysis was conducted to determine the elemental composition of the coal, this included determination of carbon, hydrogen, oxygen, sulfur and

nitrogen contents. The PerkinElmer 2400 Series II CHNS/O Elemental Analyzer shown in Figure 3.5 was used. A small quantity sample of 2 mg was accurately weighed into a small tin capsule. The sample was then combusted at elevated temperatures in presence of excess oxygen to form CO_2, H_O, SO_2 and oxides of nitrogen. The produced gases were then swept by a stream of helium gas into a reduction tube containing fine copper where nitrogen oxides were reduced to nitrogen gas and the excess oxygen removed. The gases were then collected in a mixing chamber separated by frontal chromatography and measured by thermal conductivity detectors giving output signals proportional to the concentrations.

Figure 3.5: PerkinElmer 2400 Series II CHNS/O Elemental Analyzer

The oxygen content was obtained by subtracting the sum of the four elements from 100%.

3.2.5 Gasification Process

Gasification process started by first heating charcoal inside the reactor to 650^oC, temperatures at which coal can self ignite. Coal was then fed from the top of the gasifier and air introduced from the bottom of the reactor at a controlled rate. The operation and monitoring of the gasification process involved controlling the air and coal input, monitoring the temperatures inside the reactor and gas composition. Data from this monitoring was recorded and analyzed.

3.2.6 Design of the Bed

Selection of bed height is necessary to ensure sufficiently high residence time of the coal to achieve good carbon conversion in the bed (Al-farraji, 2017). Excessive heights lead to higher pressure losses and slugging flow within reactor which causes inadequate mass transfer and can lead to mechanical failure of common support structures (Enden & Silva, 2004). Previous studies use the ratio of static height to the bed diameter as 2 for most gasifiers. However, research has shown that if this value is exceeded channeling takes place which is as a result of mesh forming properties of particles (Ramirez, Martinez, & Petro, 2007). In this research a bed height of 1.5D is adopted where D is the bed diameter. The particle size was chosen to be 3mm according to data compiled by Basu et al. (Professor Prabir Basu, 2006) which indicated that for fluidized applications the particle size should not exceed 6mm.

From the proximate analysis the density of coal was obtained as 1435 kg/m^3. Most solid particles are irregular in shape and sphericity can be estimated using expression (3.4). According to Equation 3.4 the sphericity of a sphere $\phi_s = 1$ and for other particles $0 \geq \phi_s \leq 1$.

$$\phi_s = \left(\frac{S.A_s}{S.A_p}\right) \tag{3.4}$$

S.A$_s$ represents the surface area of the sphere and S.A$_p$ represents the surface area of a particle of the same volume as the sphere.

In packed beds, the shape of particles and the particle size distribution influences heat permeability, pressure drop and heat transfer in the reactor (Ramirez et al., 2007). The sphericity of the coal particles in this research was chosen as 0.65 based on criteria by Kunii, D. and Levenspiel (Octave Levenspiel, 1991) shown in Table 3.1.

The void fraction (ε) was estimated using the following model equation developed by *Hartman et al.* (Hartman, Trnka, & Svoboda, 2000). The value was estimated as 0.55.

$$\varepsilon = 1.0 - 0.864\phi_s + 0.2745\phi_s \tag{3.5}$$

The frictional pressure drop across the bed was estimated using Ergun equation shown in Equation 3.6

$$\frac{\Delta P}{h} = 150\frac{(1-\varepsilon)^2}{\varepsilon^3}\frac{\mu u}{(\phi_s d_p)^2} + 1.75\frac{(1-\varepsilon)}{\varepsilon^3}\frac{u^2\rho_f}{\phi_s d_p} \tag{3.6}$$

Table 3.1: Sphericity of Regular and Irregular Particles (Octave Levenspiel, 1991)

Type of Particle	Sphericity
Sphere	1.00
Cube	0.81
Cylinders	
h=d	0.87
h=5d	0.70
h=10d	0.58
Disks	
h=d/3	0.76
h=d/6	0.60
h=d/10	0.47
Activated carbon and silica gels	0.70-0.90
Coal	
Anthracite	0.63
Bituminous	0.63
Natural dust	0.65
Pulverized	0.73
Magnetite, Fischer-Tropsch catalyst	0.58
Mica flakes	0.28
Sand	
Round	0.86
Sharp	0.66
Tungsten powder	0.89

where ΔP is the pressure drop, h is the height of the bed, μ is the fluid viscosity, ρ_f is the fluid density, ε is the void fraction of bed, u is the fluid velocity and d_p is the particle size.

The particles in the bed will remain in a packed bed as long as the gravitational forces holding the solid particles down are greater than the force exerted by the fluidizing air. At the point where the two equalize the solid particles begin to move up a condition referred to as incipient fluidization given by Equation (3.7)

$$\frac{\Delta P}{h} = W = (\rho_p - \rho_f)(1 - \varepsilon)g \tag{3.7}$$

where W is the weight of the fluidized particles, ΔP is the pressure drop and ρ_p and ρ_f are densities of coal particles and air respectively.

The minimum fluidization velocity (u_{mf}) was expressed as shown in Equation (3.8)

$$u_{mf} = \left[\frac{g(\rho_p - \rho_f)\varepsilon_{mf}^3 d_p}{1.75\rho_f}\right]^{\frac{1}{2}} \tag{3.8}$$

Proper fluidization occurs at a velocity called actual fluidization velocity u_f. The relationship between the minimum fluidization velocity and terminal velocity is expressed as in Equation (3.9).

$$u_{mf} < u_f < u_t \tag{3.9}$$

The fluidization velocity u_f expressed by Kozany-Carmen equation is shown in Equation (3.10)

$$u_f = \frac{(\rho_p - \rho_f)g d_p^2}{150\mu}\frac{\varepsilon^3}{1-\varepsilon} \tag{3.10}$$

The terminal velocity was estimated using Equation (3.11).

$$u_t = \frac{g(\rho_p - \rho_f)d_p^2}{18u_f} \tag{3.11}$$

3.2.7 The Reactor Design

A sizing criteria adopted by Prof. Prabrir Basu (Professor Prabir Basu, 2006) was adopted for determination of the diameter of the reactor. He proposed that the cross sectional area of the reactor can be obtained from rate of air supply required to gasify the fuel. This was done by first obtaining the stoichiometric rate of air supply required for combustion of 5 kg/h of coal which was obtained as 0.0108m^3/s as demonstrated in Appendix I;

For good gasification results the equivalence ratio ranges between 0.2 to 0.4. It then follows that the gasification air flow rate will therefore range between $2.16 \times 10^{-3} m^3/s$ to $3.78 \times 10^{-3} m^3/s$. Fluidization velocity estimates from literature for bubbling fluidized bed ranges between 0.5 to 2.5 m/s and 4 to 6 m/s for fast beds (Professor Prabir Basu, 2006). Using these velocity estimates and the gasification air flow rate the diameter of the reactor was estimated to range between 0.0214m to 0.0981m which gives a model size. A scale up was then done using a factor of 10 resulting to a diameter range of 0.214m to 0.981m. For this research a diameter of 0.255m was adopted.

The reactor was constructed of a cylindrical tube of diameter 0.315m and length of 0.5m. As the temperatures inside the gasifier can go as high as 1000^oC, the inner part of the reactor was lined with refractory clay of thickness 0.03m resulting to an inside diameter of 0.255m. The refractory was used to protect the metal

shell from abrasion by bed materials and insulate the shell from elevated temperatures (Don W. Green, n.d.). Two flanges were welded on top and bottom of the reactor to allow for connection to the freeboard section and the support structure respectively. A high temperature gasket seal (Grafoil type) was used between the flanges of the reactor and the support structure to prevent gas leakage. Bolts (M8) and washers were used to join the reactor to the bottom support structure and the upper freeboard section.

3.2.8 Design of Freeboard Section

The freeboard section was constructed of a mild steel cylindrical tube of diameter 0.38m and a length of 0.5m and a thickness 0.002m. The diameter of the freeboard section is larger than the reactor diameter by 0.065m as recommended by Ghally et al. (Ghaly & Macdonald, 2014). An increased diameter in the freeboard section is desirable as it allows for reduction of velocity of the produced gas, necessitates return of entrained particles from the bed and also provides more residence time giving complete conversion of tars to lighter hydrocarbon gases(Enden & Silva, 2004). The conversion of high molecular hydrocarbons in tars to light molecular hydrocarbon gases improves the energy content of the syngas (Jiu Huang, 2011). A feeding section was incorporated at the top of the freeboard section to allow for coal feeding. An exit pipe for the syngas was also incorporated as shown in Figure 3.2.

3.2.9 Distributor Plate Design

The distributor plate plays two main functions which include, supporting the bed material and also has holes or air caps that allow air to flow into the reactor hence initiating effective gas−solids interaction (Wormsbecker Michael, Todd s. Pugsley, 2007). Proper design of the distributor plate is important to avoid stagnant zones near the grid region which can cause hot spots resulting in agglomeration and eventual failure of the distributor (Ergudenler & Ghaly, 1993).
In this research a perforated distributor type was adopted. The distributor was designed based on requirements from Ghaly et al.(Ghaly & Macdonald, 2014), (Ghaly, Ergudenler, & Ramakrishnan, 2015). It was made of a circular steel plate of 315 mm diameter and a thickness of 3mm . A circular area of 220mm diameter was perforated with perforation area being 1.63% of the bed cross-sectional area(255mm). A total of 267 holes of 2mm diameter each were drilled using a triangular pitch of 11.1mm as shown in Figure 3.6.

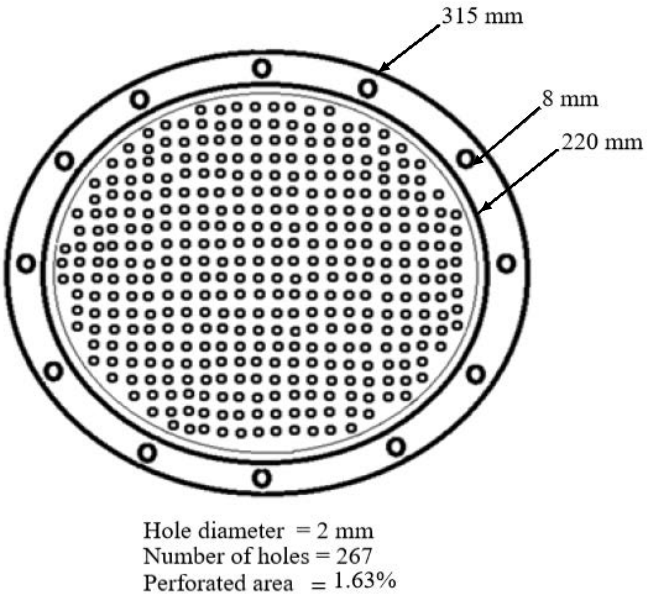

Figure 3.6: Distributor plate

3.2.10 Support Structure and The Plenum.

The support stand was constructed of 50mm mild steel angle line bars. It consisted of a square top structure (415mm) supported by four 450mm long L section bars as shown in Figure 3.7 below.

Figure 3.7: Support structure for the reactor

3.3 The Air Supply System

The air supply system consisted of a blower and a piping of diameter 50.8 mm connecting the blower and the plenum section of the support structure. The blower was rated at 600W and with a maximum flow rate of 3.5m^3/min. The power rating of the blower was computed by multiplying the pressure drop and air flow rate in the reactor as shown in Equation 3.12

$$Pw = \Delta P \times Q \tag{3.12}$$

where Pw is the power rating of the blower, ΔP is the pressure drop across the bed and Q is the air flow rate in the reactor.

The blower had provision to vary the flow rate through six levels with the sixth level corresponding to 3.5m^3/min. To obtain the flow rates at the other five levels the blower was calibrated using an Air Flow Bench shown in Figure 3.8 This was done by fitting the blower on one end of the bench as shown in Figure

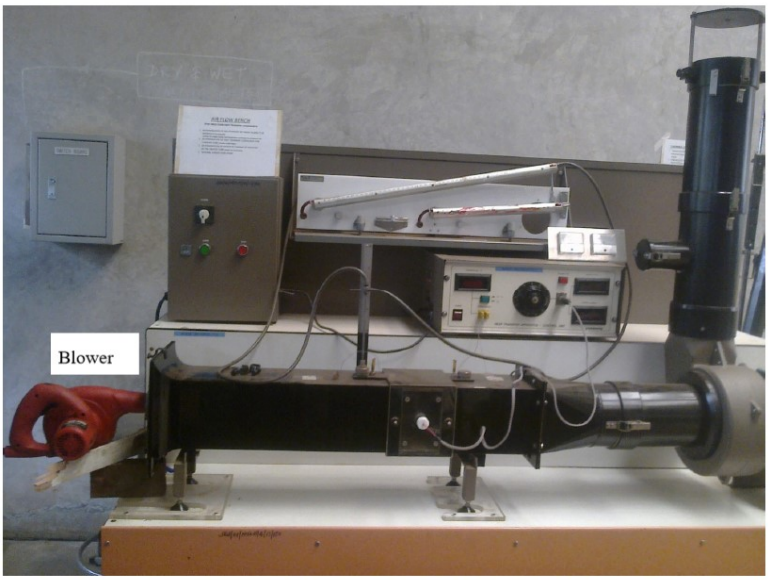

Figure 3.8: The Air Flow Bench Apparatus used for Blower Calibration

3.8. A single mercury test module with a tube of 12.7 mm diameter in position was then fitted into the duct and coupled to the bench control unit. The bench heater was switched on and the output adjusted until a temperature difference of 20^oC was achieved. The reading on the mercury tube was then recorded at this temperature difference and the procedure was repeated for all blower levels. The flow rates at different levels were computed from the recorded readings.

3.4 Performance Parameters

The Bench scale gasifier fabricated was tested for performance by testing the syngas composition at various air flow rates (0.5,1.0,1.5,2.0) m^3/ min during gasification. The composition components tested were CO, CO_2, H_2, No_x and SO_2 emissions and among these gases, the fuel elements are CO and H_2. The syngas outlet temperature at the free board section was also tested. The feeding pressures and the reactor temperatures were also tested at different air flow rates during gasification and the experimental tests are presented below.

3.4.1 Fuel Heating Value (Calorific Value)

The fuel heating value or the calorific value is the amount of heat released per unit mass or per unit volume of the fuel when it is completely burnt in air at standard conditions (STP) (25^oC and 101.3kPa) (Sara Mcallister, Jyh-Yuan Chen, n.d.). It is expressed in MJ/Kg and can either be Higher heating Value (HHV) or Lower Heating Value(LHV) depending on whether water in the products is in liquid or gaseous state respectively. HHV is achieved when no energy is used to vaporize the water present in the combustion products meaning the water is in liquid state. HHV therefore comprises of both sensible heat energy and latent heat of vaporization. LHV on the other hand results when all water in the combustion products is vaporized and therefore it contains only sensible heat energy. Any analysis involving heating value utilizes LHV.

HHV was determined experimentally using constant volume process in an auto adiabatic bomb calorimeter, GallenKamp type with an accuracy of +5%. Shown in Fig.3.9 is the photographic view of the bomb calorimeter used. It had a pressure tight combustion chamber where O_2 was charged into the chamber at a pressure of 30 bar.

A steel chamber was immersed into another cylindrical container having its weight and water in it adding up to 3.0 kg. HHV was then determined by completely burning 0.5 grams of coal in the confined combustion chamber full of O_2 at 30.0 bar as indicated above. A 90.0 mm thread was used in the combustion chamber to initiate ignition of coal. Combustion products were cooled to ambient conditions to condense any water vapour present in the combustion products. HHV was then estimated using Equation 3.13 as shown:

$$HHV = \frac{(K_1 \Delta T) - K_2}{m_s} \tag{3.13}$$

where ΔT is the difference between initial and final temperature of burned sample,

Figure 3.9: Constant Volume Bomb Calorimeter

m_s is the mass of the sample burned, K_1 is the bomb calorimeter constant whose value is 10.35 and K_2 is the energy for the 90.0 mm thread whose value is 0.126. Moisture content in the coal was determined by drying method and its value used to calculate the latent heat of vaporization of water in the coal. LHV was then calculated using Equation 3.14

$$LHV = HHV(1 - M) - 2.447M \tag{3.14}$$

Where M is the wet basis moisture content and 2.447 is the latent heat of vaporization of water in MJ/Kg at 25^oC.

3.4.2 Syngas Composition Test

Composition is of major importance as it helps in determination of the quality of syngas produced. Syngas composition is influenced by many parameters ranging from the fuel type, the gasifying agent and its flow rate, the type of gasifier among others. In this case a fluidized bed gasifier is used, the fuel being sub-bituminous coal and air as the gasifying agent. The composition of the syngas produced was determined using Testo 350-S/-XL gas analyzer with an accuracy of $\pm 5\%$. Testo 350-S/-XL gas analyzer shown in Figure 3.10 is a flexible portable analysis system which comprises of a control unit, a flue gas analyzer and and gas probe. The gas analyzer is fitted with sensors for NO, NO_2, SO_2, CO, CO_2 and H_2.
During measurement, the probe was inserted in the syngas outlet to draw in

Figure 3.10: Gas Analyzer

syngas and the results were displayed on the analyzer screen. The analyzer gives the composition in ppm (parts per million) and Equation 3.15 was used to convert the composition of individual components to a percentage where A is 1,000,000.

$$x(\%) = \frac{x(ppm)}{A}100 \tag{3.15}$$

3.4.3 Temperature Measurement

During fabrication of the gasifier provisions were included on the bottom, middle and top of the reactor to allow for temperature measurement. Temperature measurement was done using Gispo-d immersion thermometer shown in Figure 3.11 and k-type thermocouples. Gispo-d is made of Nicr-Ni element with measuring range of -50^oC to $+1350^oC$ and accuracy of $\pm 1^oC \pm 0.2\%$ of the measured value.

The K-type thermocouples were threaded to allow for better fitting on the gasifier and had a probe for measuring the temperature as shown in Figure 3.12. The cables of the thermocouples were coupled to a data logger model TDS-530 shown in Figure 3.13. The data logger response time was 0.4 s. The accuracy of the data logger is dependent on the accuracy of the thermocouples attached.

3.4.4 Safety

Carbon monoxide forms one of the major components of syngas. Its a highly poisonous gas if inhaled it can lead to unconsciousness or even death when first

Figure 3.11: Gispo-d Immersion Thermometer

Figure 3.12: K-Type Thermocouple

Figure 3.13: TDS-530 Data Logger

aid is not given immediately (Industrial Accident Prevention Association 2008., 2008). CO is highly flammable and leakages can cause explosions and this makes control of leakages important in gasification processes (Europe, n.d.). To avoid all these, the rig was set up in fully ventilated section and also gas masks were used to minimize the inhalation of CO.

Figure 3.14: Ultrasonic Leak Detector

Also conducted was the leaking test. The gasifier setup had several joints along the air intake and the gasifier. The joints between the suction line and the plenum, the plenum and the reactor, the reactor and the free board section were fastened together using nuts secured with gasket seals. The leakage test was done using ultrasonic leak detector, model number GS-5800 shown in Figure 3.14. The blower was switched on and the points of leakage were identified by placing the the sensor horn of the detector on the joints at different angles for better results. In presence of leakages, the level of audible ultrasonic sound and level on the LED display panel changed.

3.5 Estimation of Coal Gasification Chemical Equation

Coal is a complex solid fuel containing C, H, O, N and S in varying compositions. CH_mO forms the basic part of the fuel. Gasifying the coal using atmospheric air

as the gasifying agent yields a LHV syngas containing 5 principal components with around 50% nitrogen on volume basis, some quantities of hydrogen, carbon monoxide (combustible), carbon dioxide and some traces of methane. The gasification equation can be written as follows;

$$x_1C_{5.453}H_{4.6}O_{0.489}+x_2(O_2+3.76N_2) \rightarrow x_3CO+x_4CO_2+x_5H_2+x_6CH_4+3.76x_2N_2 \tag{3.16}$$

Using the compositions of syngas obtained and doing molar balances for each element in Equation 3.16, the global gasification coefficients were obtained for the different air flow rates as shown below:

Air flow rate of 0.5m^3/s
$C_{5.453}H_{4.6}O_{0.489}+1.795(O_2+3.76N_2) \rightarrow 2.782CO+2.048CO_2+1.296H_2+0.624CH_4 + 6.749N_2$

Air flow rate of 1.0m^3/s
$C_{5.453}H_{4.6}O_{0.489}+1.797(O_2+3.76N_2) \rightarrow 3.014CO+1.921CO_2+0.941H_2+0.512CH_4+ 6.757N_2$

Air flow rate of 1.5m^3/s
$C_{5.453}H_{4.6}O_{0.489}+2.194(O_2+3.76N_2) \rightarrow 2.693CO+2.293CO_2+1.022H_2+0.467CH_4+ 8.25N_2$

Air flow rate of 2.0m^3/s
$C_{5.453}H_{4.6}O_{0.489}+2.285(O_2+3.76N_2) \rightarrow 2.630CO+2.401CO_2+0.842H_2+0.422CH_4+ 8.5N_2$

3.6 Equivalence Ratio

Equivalence ratio is the ratio of actual fuel-air ratio to the stoichiometric (theoretical air) fuel-air ratio. The equivalence ratio for the gasification process was obtained using Equation 3.17

$$\phi = \frac{m_f/m_a}{m_f/m_{as}} = \frac{m_{as}}{m_a} \tag{3.17}$$

where ϕ is the equivalence ratio, m_f is the mass of the fuel, m_a is the mass of actual air used and m_{as} is the theoretical air.

3.7 Higher Heating Value (HHV) of Syngas

The HHV also called the gross calorific value (GCV) of the syngas is determined from the combustible constituent gases which include CO, H_2 and CH_4. The calorific value was computed using the compositions of the combustible gases measured and estimates of HHV of individual gases by Lars et al. (Lars Waldheim, 2001). The following Equation 3.18 was used to obtain the syngas HHV.

$$HHV_{sy} = y_{H_2} HHV_{H_2} + y_{CO} HHV_{CO} + y_{CH_4} HHV_{CH_4} \tag{3.18}$$

3.8 Cold Gas Efficiency (CGE) and Carbon Conversion (CC)

Cold gas efficiency and carbon conversion are indices used to evaluate the performance of a gasification process (W.-h. Chen, Chen, Hung, Shen, & Hsu, 2013). CGE refers to the ratio of the energy content of the syngas produced and the energy content of the fuel fed in the gasifier (Shakorfow, 2016). The energy content of the syngas was obtained by multiplying the net HHV of the syngas and its flow rate, whereas the energy content of the coal was obtained by multiplying the HHV of coal and its consumption rate as shown in Equation. 3.20. CGE is determined from concentrations of H_2, CO and CH_4

$$CGE(\%) = \left(\frac{\dot{m}_{out} \left(y_{H_2} HHV_{H_2} + y_{CO} HHV_{CO} + y_{CH_4} HHV_{CH_4} \right)}{\dot{m}_{in\,F} HHV_F} \right) \times 100 \tag{3.19}$$

where $\dot{m}_{out}$ is the mass flow rate of the syngas, $\dot{m}_{in\,F}$ is the fuel consumption rate, y_i is the mole fraction indices of species i in the product gas obtained from Equation 3.16 and HHV is the higher heating value of the respective constituents of the syngas shown in Table 3.2. The HHV of constituent gases of the syngas used to calculate the syngas heating value are as outlined in Table 3.2 (Lars Waldheim, 2001)

Table 3.2: HHV of Gases in MJ/Nm^3.

Type of Gas	HHV
CO	12.745
H_2	12.633
CH_4	39.819

Carbon conversion is the ratio of fuel carbon which is converted into non-condensable gaseous carbon components to the total fed carbon. CC is evaluated from concentrations of CO_2, CO and CH_4 as shown;

$$CC(\%) = \left(1 - \frac{\dot{m}_{out}(y_{CO_2}\frac{12}{44} + y_{CO}\frac{12}{28} + y_{CH_4}\frac{12}{16})}{\dot{m}_{inF}y_C}\right) \times 100 \tag{3.20}$$

3.9 Uncertainty

3.9.1 Background

A statement of uncertainty indicates how large the measurement error might be or simply it refers to the margin that exists about the result of any measurement. Usually all measurements are wrong in that, the measured value (result) and the right answer (true value) are different. The difference between the two is the measurement error. Unfortunately, the true value is never precisely known and by the same token neither is the measurement error. To quantify uncertainty, one needs to state the width of the margin or interval and the confidence level as a percentage as shown in Equation 3.21. Unless stated the confidence level is normally taken as 95%.

$$T = T_m \pm U_T \tag{3.21}$$

Where T is the true value T_m is the measured value and U_T is the measurement uncertainty. Evaluation of uncertainty is by statistical calculation from a series of repeated observations as one measurement alone is never enough. It is essential to repeat the procedure and average the results. The advantage of taking the mean value is that the variations in such influences will tend to be nullified. It is then possible to get the standard deviation of their mean which is known as the standard uncertainty of the mean.
The fabricated bench scale gasifier was tested for performance and data was collected using equipments like the TDS-530 data logger, gas analyzer and thermocouples . The coal HHV was also estimated using a constant volume bomb calorimeter. The tests in each case involved several measurements and their mean and standard deviation were evaluated.

3.9.2 Instrumental Uncertainty

This refers to the uncertainty arising from fluctuations in readings of the instrument scale either because the settings are not exactly reproducible due to imperfections in the equipment or because of human imperfection in observing setting or a combination of both. Instruments of varied accuracy and precision were used during data collection while testing the performance of the bench scale

gasifier. Bevington and Robinson (Philip R. Bevington, 2003) proposed a technique with a propagation equation to estimate these uncertainties. This technique was applied by Owiti (Bernard Owiti, 2015) in obtaining instrumentation random uncertainties during testing of a Waste Lubrication Oil burner rig for process heating in small to medium enterprises.

The performance of the bench scale gasifier involved the determination of the reactor temperatures at different air flow rates, composition of the syngas produced, carbon conversion and the cold gas efficiency (CGE). The CGE of the gasification process constituted the syngas higher heating value, coal higher heating value, mass flow rates of the fuel and the syngas produced and composition of the syngas produced as shown in Equation 3.22.

$$CGE\% = CGE(\dot{m}, \dot{m}_f, y_i, HHV_{fuel}, HHV_{syngas}) \tag{3.22}$$

The uncertainty was expressed using the general Equation 3.25

$$\sigma_{CGE} = \sqrt{\left(\frac{\delta_{CGE}}{\delta\dot{m}}U_{\dot{m}}\right)^2 + \left(\frac{\delta_{CGE}}{\delta y_i}U_{y_i}\right)^2 + \left(\frac{\delta_{CGE}}{\delta_{HHV_F}}U_{HHV_F}\right)^2 + \left(\frac{\delta_{CGE}}{\delta_{HHV_{sy}}}U_{HHV_{sy}}\right)^2} \tag{3.23}$$

where $U_{\dot{m}}$, U_{yi}, U_{HHV_F} were the uncertainties from the respective measuring instruments (weighing scale and a stop watch, gas analyzer and a bomb calorimeter). Mass flow rate was measured using more than one equipment and the propagated uncertainty was computed as follows

$$\dot{m} = \frac{mass}{time} = \frac{m}{t} \tag{3.24}$$

in this case a weighing scale and a stop watch were used with manufacturer's accuracies specified as ± 0.1 grams ($\sigma_m = \pm 0.1g$) and ± 0.1 seconds ($\sigma_t = \pm 0.1s$) respectively. The uncertainty equation for the fuel flow rate is then expressed as

$$\sigma_{\dot{m}} = \sqrt{\left(\frac{\delta_{\dot{m}}}{m}\sigma_m\right)^2 + \left(\frac{\delta_{\dot{m}}}{t}\sigma_t\right)^2} \tag{3.25}$$

The partial derivatives of the fuel flow rate with respect to mass and time are given as;

$$\frac{\delta_{\dot{m}}}{\delta_m} = \frac{\delta}{\delta_m}\left(\frac{m}{t}\right) = \frac{1}{t} \tag{3.26}$$

$$\frac{\delta_{\dot{m}}}{\delta_t} = \frac{\delta}{\delta_t}\left(\frac{m}{t}\right) = -\frac{1}{t^2} \tag{3.27}$$

Hence;

$$\sigma_{\dot{m}} = \pm\sqrt{\left(\frac{1}{t}\sigma_m\right)^2 + \left(-\frac{m}{t^2}\sigma_t\right)^2} \tag{3.28}$$

Expressing the uncertainty as relative to the values measured gives

$$\frac{\sigma_{\dot{m}}}{\dot{m}} = U_{\dot{m}} = \pm\sqrt{\left(\frac{\sigma_m}{m}\right)^2 + \left(\frac{-\sigma_t}{t}\right)^2} \tag{3.29}$$

and in percentage;

$$U_{\dot{m}} = 100X\sqrt{\left(\frac{\sigma_m}{m}\right)^2 + \left(-\frac{\sigma_t}{t}\right)^2} \tag{3.30}$$

Writing Eqn. 3.25 as a percentage gives Equation. 3.31

$$\frac{\sigma_{CGE}}{CGE} = 100\sqrt{\left(\frac{\sigma_{\dot{m}}}{\dot{m}}\right)^2 + \left(\frac{\sigma_{yi}}{y_i}\right)^2 + \left(\frac{\sigma_{HHV_F}}{HHV_F}\right)^2 + \left(\frac{\sigma_{HHV_{sy}}}{HHV_{sy}}\right)^2} \tag{3.31}$$

$$U_{CGE} = 100\sqrt{(U_{\dot{m}})^2 + (U_{y_i})^2 + (U_{HHV_F})^2 + \left(U_{HHV_{sy}}\right)^2} \tag{3.32}$$

From Eqn. 3.31 and Equation. 3.32 the uncertainty of the cold gas efficiency was determined as 0.35 %. Based on confidence level of 95 % the uncertainties calculated should not exceed 5 % and therefore the value was within range of accuracies of the instruments used.

3.9.3 Experimental Uncertainty

Experimental uncertainty refers to the deviation from the mean of the collected results under similar conditions. To quantify experimental uncertainty the spread of the values has to be estimated. The best method to quantify spread is standard deviation denoted by symbol σ as proposed by Stephanie Bell (Bell, 2001) using expression 3.33. The coefficient of variation (COV) can also be used to measure the variability of the obtained data relative to its mean as shown in Equation. 3.34.

$$\sigma = \sqrt{\frac{\sum_{i=1}^{n}(x_1 - \bar{x})^2}{n-1}} \tag{3.33}$$

$$COV = \frac{\sigma}{\bar{x}} \tag{3.34}$$

where i^{th} is the number of repeated measurement, n is the results considered, x^i is the result of the i^{th} measurement and $\bar{x}$ is the arithmetic mean. The arithmetic mean of the measured data was obtained using expression 3.35 shown

$$\bar{x} = \frac{1}{n}(x_1 + x_2 + ...x_n) \tag{3.35}$$

Expressing Eqn. 3.33 as a percentage gives

$$\sigma = 100 \times \frac{\sqrt{\frac{\sum_{i=1}^{n}(x_1 - \bar{x})^2}{n-1}}}{\bar{x}} \tag{3.36}$$

CHAPTER FOUR
RESULTS AND DISCUSSION

4.1 Background

In this chapter the test results, the analysis and the discussions of the obtained parameters for the fluidized bed coal gasification in a bench scale gasifier are presented. The cold gas efficiency and the carbon conversion of the gasifier under different flow conditions are also presented.

4.2 Coal Analysis

4.2.1 Proximate Analysis

The results from proximate analysis of the coal samples are presented in the Table 4.1.

Table 4.1: Proximate Analysis Results for Coal

Coal Property	**Average Value**
Bulk Density	1.4347 g/cm^3
Moisture Content	4.09%
Ash Content	13.99%
Calorific Value	30.443MJ/Kg
Fixed Carbon	42.62%

The calorific value was obtained was above 30MJ/kg, from a bomb calorimeter and this corresponds to the Higher Heating Value (HHV) of the coal as the water was condensed. The calorific value of coal sample obtained is higher compared to that of low rank coal (lignite) coal which is about 21.65MJ/kg. High rank coal (anthracite) on the other hand has calorific value of around 34.6MJ/kg (Carvill, 1993).

The moisture content of 4.09% was obtained which is minimal as most low rank coals have moisture content of between 30% and 70% (Krawczykowska & Marciniak-kowalska, 2012). The low moisture content is desirable as less heat would be required to vaporize the water during gasification. A study by Bullinger *et al.* (Bullinger, Ness, Dakota, Sarunac, & Levy, 2002) on effects of coal drying on performance of boilers as pertains moisture content on lignite coal showed that about 7% of the fuel heat input in boilers is used to evaporate the moisture. In their study, drying the lignite coal to moisture content of 10-15% was found to improve the efficiency of the energy blocks by 4-6%.

The fixed carbon content obtained from the experiment was 42.62% and this classifies coal used in this research as sub-bituminous as shown in Table 4.2.

Table 4.2: Coal Classification (Miller & Tillman, 2008).

Coal Type	Fixed Carbon (%)
Anthracite	85-98
Bituminous	45-85
Sub-bituminous	35-45
Lignite	25-35

4.2.2 Ultimate Analysis

The results from ultimate analysis of the coal samples are presented in and Table 4.3. From the ultimate analysis the fuel components were identified as carbon,

Table 4.3: Ultimate Analysis Results for Coal

Constituents	**% by weight (kg)**
Carbon	65.44
Hydrogen	4.6
Oxygen	7.82
Nitrogen	1.07
Sulphur	3.61

hydrogen and oxygen as shown in Table 4.3. The other components like nitrogen and sulphur are impurities which form part of the emissions during gasification.

4.3 Effect of air flow rate on product distribution

In this analysis the air flow rate was varied while keeping the fuel feed rate constant. The results are presented in Figure 4.1 and Table C.1. From Figure 4.1, it can be seen that the concentration of CO first increased by 2.31% then started to decrease. Increasing air flow rate increases the amount of oxygen required for exothermic reactions as shown in reaction Equations 2.1, 2.2 and 2.3.These reactions raise the temperatures of the reactor. This provides a conducive environment for reaction Equations 2.4 (steam decomposition) and 2.6 (carbon reduction) thus increasing the amount of CO by 2.31%. Increasing the air flow rate provides more oxygen which oxidizes CO to CO_2 and that explains behaviour of the CO curve after 1.5m^3/min flow rate.

On the other hand, the concentration of CO_2 decreased first then it started to increases as the air flow rate was increased further. Increasing the air flow rate further provides more oxygen and most of the carbon is converted to CO_2 and some of the CO gets oxidized to CO_2, hence the curve of CO_2 tends to increase

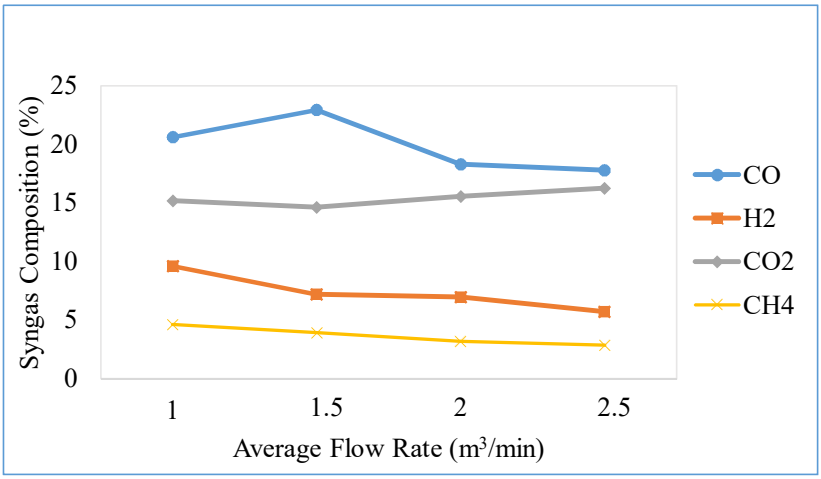

Figure 4.1: Syngas composition variations at different air flow rates

with an increase with air flow rate. The concentrations of hydrogen decreases with increase in air flow rate.

Hydrogen concentrations remained significantly low throughout the tests for this research, this was also noted by P.J *Ashman et al.* (Ashman, Kosminski, Button, & Mullinger, 2005) when they compared composition of syngas from air/steam gasification and air only gasifications. Methane concentrations are seen to decrease slightly with increase of air flow rate. This is because methane gas gets oxidized to carbon dioxide and water due to reaction with oxygen.

4.4 Effect of Air Flow Rate on Syngas Output Temperature

The temperature of the syngas leaving the gasifier was found to increase by 203^oC with increase of air flow rate upto 2.0m^3/min and then it started to reduce as shown in the curve in Figure 4.2.

Increasing the air flow rate increases the amount of oxygen and this means carbon oxidation reactions will be favoured and since the reactions are exothermic the reactor temperatures go up and thus higher temperature at outlet. The highest outlet temperature obtained was above 577^oC which is within range as syngas outlet temperatures from literature range between 400^oC to 1600^oC (Zhu, 2015). When the reactor temperatures are high it follows that output syngas will be at a higher temperature. The high temperatures of the syngas at the outlet shows trapped heat energy. This heat can be recovered for steam generation and process heating. For the application of the syngas in gas turbine or internal com-

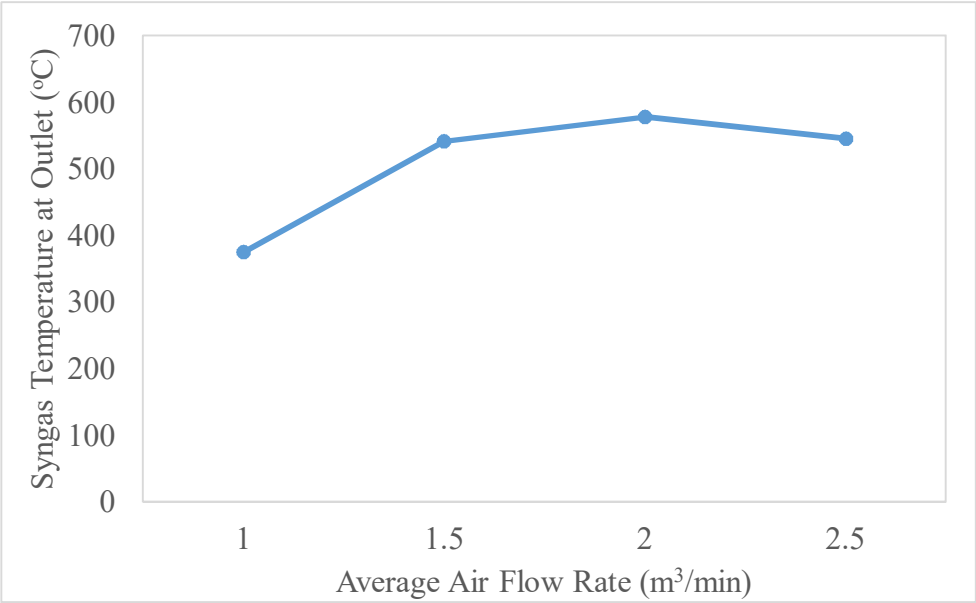

Figure 4.2: Syngas outlet temperature variation with air flow rate

bustion engine cleaning is required to remove water vapour, sulfur compounds, particulate matter and tars. To do so, cooling of the syngas is necessary. This is because the cleaning processes are carried out at low temperatures; less than 500^oC for solid particulates and almost ambient temperatures for acid gases and other contaminants (Zhu, 2015).

4.5 Effect of Air Flow Rate on Emissions

Any combustion process is rated clean or unclean depending on the levels of emissions. From the curve in Figure 4.3 it can be seen that the NO_x levels increased with increase of air flow rate.The SO_2 levels also increased slightly with increase in the air flow rate. NO_x is formed from reaction of nitrogen in air and oxygen and this reaction is dependent on prevailing temperatures as it requires high temperatures. Increasing the air flow rate led to increase in reactor temperature and that explains the increase in NO_x levels from 60ppm to 110ppm. SO_2 emissions on the other hand depend on the amount of sulfur in the fuel and since the amount of sulfur in the fuel is significantly small in this case 3.61% the increase in SO_2 levels with increasing air flow rate is also small as shown in Figure 4.3.

The threshold limit value (TLV) for NO_x is 200 mg/m^3 (106 ppm) while that of SO_2 is 200 mg/m^3 (106 ppm) in European Union, China and Japan (Zhang, 2016). The TLV from the curve it can be seen that the NO_x exceeded its TLV

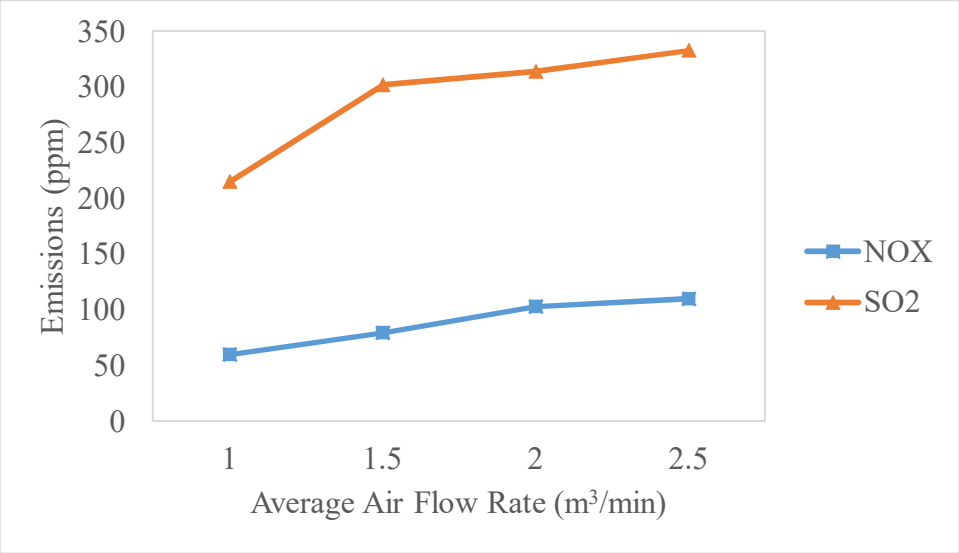

Figure 4.3: NO_x and SO_2 emissions at various air flow rates

value at airflow rate beyond 1.5 m^3/min while the SO_2 levels exceeded the TLV value. Both NO_x and SO_2 are acidic gases and they react with water droplets in the atmosphere forming acid rain which can harm ecosystems. Inhaling large concentrations of this gases can irritate airways in human respiratory system and aggravate diseases like asthma. NO_x reacts with compounds in the atmosphere forming nitrite particles that form smog which reduces visibility. SO_2 on the other hand reacts with compounds in the atmosphere to form sulphate particles that form part of particulate matter which impairs visibility. This means for the syngas to be used in any combustion application clean up processes to remove the NO_x and SO_2 are necessary.

The levels of NO_x and SO_2 emissions from this research have exceeded the TLV and for the syngas to be utilized in any combustion process for example, measures have to be put in place to clean up the syngas.

4.6 Effect of Air Flow Rate on Heating Value of Syngas

As the air flow rate was varied the HHV of the output syngas was noted to decrease from 5.667MJ/Nm^3 to 4.106MJ/Nm^3 as shown in Figure 4.4 and Table C.3. From the curve it can be seen that the HHV is relatively high for the first two flow rates.

The calorific value of the syngas is dependent on the concentration of the combustible gases (CO, H_2 and CH_4), increasing the air flow rate was noted to increase the concentrations of CO between air flow rates 1-1.5m^3/min and this explains

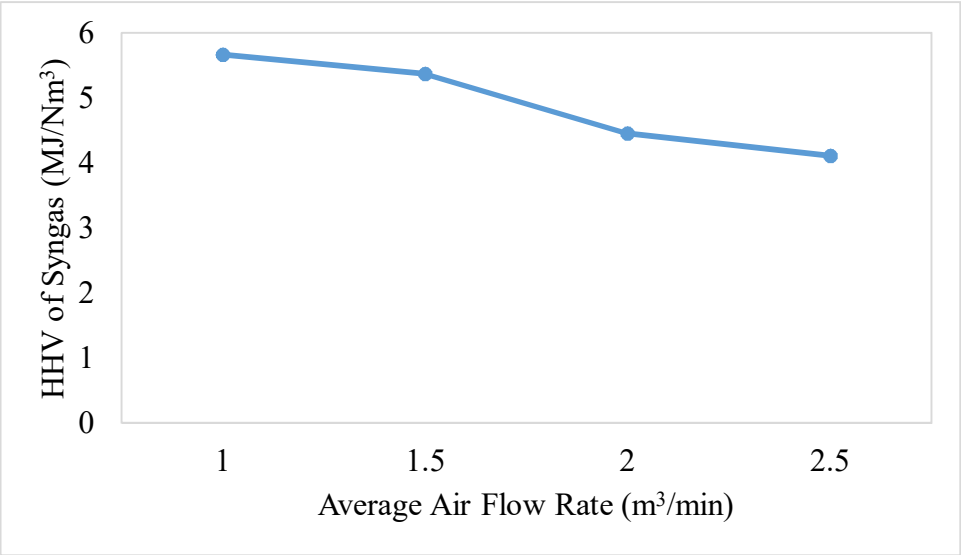

Figure 4.4: Syngas calorific value variations with air flow rate

the relatively high HHV. Increased concentration of N_2 which is non combustible in the syngas as the air flow rate was increased further explains the decrease in the HHV of the syngas. The behaviour was found to be similar to what was reported by Daniela et al.(Tasma & Uzunanu, 2007).
The optimal air flow rate for the gasification process was obtained as 1.5 m^3/min which corresponds to an equivalence ratio of 0.283. At this equivalence ratio the HHV of the syngas was above 5MJ/Nm^3.

4.7 Effect of Air flow Rate on the Reactor Temperature

The reactor temperature was seen to increase with increasing air flow rate as seen in Figure 4.5.
Increasing the air flow rate increases the amount of oxygen available for combustion reactions Equations 2.1, 2.2 and 2.3 which are exothermic and that explains the temperature increase from 850^oC to 873^oC.

4.8 Cold Gas Efficiency and Carbon Conversion Efficiency

The cold gas efficiency and the carbon conversion efficiency of the gasifier at the corresponding air flow rates were determined and the results are tabulated in Table 4.4. The highest CGE obtained for this research was 65.92%. From literature review the CGE for oxygen blown gasifiers is $\geq$ 80% (Seo et al., 2011). The low CGE for this research was because of high nitrogen concentrations in the

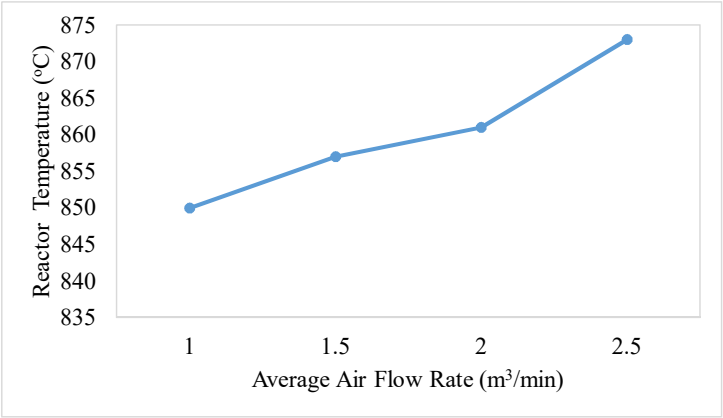

Figure 4.5: Reactor temperature variation with air flow rate

syngas that lowered its heating value. The highest carbon conversion efficiency was obtained as 89.89%.

Table 4.4: Cold Gas and Carbon Conversion Efficiencies

Air Flow Rate (m^3/min)	1.0	1.5	2.0	2.5
CGE (%)	65.92	62.66	60.16	57.11
CCE (%)	88.00	89.89	86.63	86.42

CHAPTER FIVE
CONCLUSIONS AND RECOMMENDATIONS

5.1 Conclusions

In this research, a bench scale gasifier was designed and fabricated. Both the ultimate and proximate analysis of coal were determined. Performance tests of the gasifier were conducted by varying various parameters and the results were monitored and recorded.
From the analysis of the results obtained from the experiments, the following conclusions were deduced;

- Gasification of coal in small scale is possible and the syngas obtained can be used for domestic use like cooking, and running of small engines.
- The calorific value of coal was found to be over 30MJ/Kg which classifies the coal used as sub-bituminous. This shows that coal has high energy density and it will continue to be used as source of energy.
- Syngas composition was noted to vary with increase of air flow rate.The highest HHV of the syngas obtained was over 5MJ/Nm^3 which led to the conclusion that the syngas produced can be used as fuel in gas turbine applications.
- Reactor temperatures of above 800^oC achieved indicate the capability of the bench scale gasifier to supply process heat for steam boilers, restaurants, hotels among others.
- Emissions from coal gasification are influenced by both temperature and air flow rate. NO_x and SO_2 emissions increased with increase in air flow rate.

Fluidized bed gasification of coal can be a reliable source of energy to supplement other sources of energy in our country Kenya as country tries to achieve vision 2030.

5.2 Recommendations

From this research,results and discussions the following recommendations for later study are suggested:

- Coal gasification produces non combustible elements like CO_2, SOx and NOx which are harmful to the ecosystem. The nitrogen concentrations in the syngas was observed to be almost 50% on volume basis and for

applications of the syngas as fuel purification is necessary. Clean up and purification of the syngas is extensive and should therefore constitute an independent research.

- Too much heat is emitted from the gasification process due to the high temperatures. A research on how to use this heat for process heating for example in steam generators is needed.

- Syngas produced from the gasification process can used as fuel owing to its high HHV therefore, research on the combustion characteristics of the syngas is therefore critical.

- Gasifiers are flexible when it comes to the feedstocks, future improvements can include gasification of other solid fuels or co-gasification of coal with other solid fuels like biomass.

REFERENCES

Abdulganiyu, I., Honkapuro, S., & Annala, S. (2017). *Assessing the Potential and Barriers of Renewable Energy Market in Developing Countries: The Case of Kenya* (Tech. Rep.).

Adaptation, V., & Var, R. (2009). Energy Systems : Mali. (33), 1–41.

Al-farraji, A. A. M. (2017). *Chemical Engineering and Reactor Design of a Fluidised Bed Gasifier* (Unpublished doctoral dissertation).

Amu Power Company Limited. (2016). *1 , 050MW Coal Fired Power Plant Stakeholder Engagement Plan* (Tech. Rep. No. July).

Andreeva, D., Idakiev, V., Tabakova, T., Ilieva, L., Falaras, P., Bourlinos, A., & Travlos, A. (2002). Low-temperature water-gas shift reaction over Au / CeO 2 catalysts. *Catalysis Today*, *72*, 51–57.

Ashman, P. J., Kosminski, A., Button, S. J., & Mullinger, P. J. (2005). Gasification of Victorian Lignite in a Laboratory Scale Fluidised Bed Gasifier . *5th Asia-Pacific Conference on Combustion*(July), 18–20.

Ayodele, V., Offor, U. H., Akhabue, E., Akhihiero, T., & Cheng, C. K. (2017). Hydrogen Production From catalytic reforming of greenhouse gases (CO 2 and CH 4) Over Neodymiun (III) oxide supported Cobalt catalyst. *Appl. Sci. Environ. Manage*, *21*(6), 1051–1056.

Bell, S. (2001). *Good Practice Guide A Beginner ' s Guide to Uncertainty of* (Tech. Rep. No. 2). Teddington, Middlesex, United Kingdom, TW11 0LW.

Bernard Owiti. (2015). *Performance of waste Lubrication Oil Burner for Process Heating in Small to Medium Enterprises* (Unpublished doctoral dissertation). JKUAT.

Bohm, M. C., Herzog, H. J., Parsons, J. E., & Sekar, R. C. (2007). Capture-ready coal plants Options , technologies and economics. *International Journal of Greenhouse Gas Control*, *1*(X), 113–120.

Breault, R. W. (2010). Gasification processes old and new: A basic review of the major technologies. *Energies*, *3*(2), 216–240.

Bullinger, C., Ness, M., Dakota, N., Sarunac, N., & Levy, E. K. (2002). Coal Drying Improves Performance and Reduces Emissions. *International technical Conference on Coal Utilization & Fuel Systems*.

Calin-Cristian Cormos, P. S. A., & Babes. (2012). Integrated assessment of carbon capture and storage technologies in coal based power generation using CAPE tools. In *Computer aided process engineering* (pp. 56–60).

Campbell, P. E., McMullan, J. T., & Williams, B. C. (2000). Concept for a competitive coal fired integrated gasification combined cycle power plant. *Fuel*, *79*(9), 1031–1040.

Carvill, J. (1993). Thermodynamics and Heat Transfer. In *Mechanical engineer's data hand book* (pp. 102–145).

CENCERE(Centre for Clean Energy Research and Education). (n.d.). *HHV of Syngas* (Tech. Rep.). Eastern Illinois University.

Chang, S., Zhuo, J., Meng, S., Qin, S., & Yao, Q. (2016). Clean Coal Technologies in China: Current Status and Future Perspectives. *Engineering*, *2*(4), 447–459.

Chen, C., Horio, M., & Kojima, T. (2000). Numerical simulation of entrained flow coal gasifiers. Part II: Effects of operating conditions on gasifier performance. *Chemical Engineering Science*, *55*(18), 3875–3883.

Chen, W.-h., Chen, C.-j., Hung, C.-i., Shen, C.-h., & Hsu, H.-w. (2013). A comparison of gasification phenomena among raw biomass , torrefied biomass and coal in an entrained-flow reactor. *Applied energy*, *112*, 421–430.

Chmielniak, T., & Sciazko, M. (2003). Co-gasification of biomass and coal for methanol synthesis. *Applied energy*, *74*, 393–403.

Choi, Y. C., Li, X. Y., Park, T. J., Kim, J. H., & Lee, J. G. (2001). Numerical study on the coal gasification characteristics in an entrained flow coal gasifier. *Fuel*, *80*.

Couto, N., Rouboa, A., Silva, V., Monteiro, E., & Bouziane, K. (2013). Influence of the biomass gasification processes on the final composition of syngas. *Energy Procedia*, *36*, 596–606.

Dayananda, B. S., & Sreepathi, L. K. (2012). Design and Analysis of Fluidized Bed gasifier for Chicken Litter along with Agro Wastes. *International Research Journal of Environment Sciences*, *1*(3), 11–16.

Dechsiri, C. (2004). *Particle Transport in Fluidized Beds Experiments and Stochastic Models* (Unpublished doctoral dissertation). University of Groningen Particle.

Doerell, P. E. (1999). All future energy will have to be clean. *Applied Energy*, *64*(1-4), 79–88.

Don W. Green, R. H. P. H. N. (n.d.). *Perry's Chemical Engineers'Handbook*.

Enden, P. J. V. D., & Silva, E. (2004). Design approach for a biomass fed fluidized bed gasifier using the simulation software CSFB. *Biomass & Bioenergy*, *26*, 281–287.

Engelbrecht, a. D., North, B. C., Oboirien, B. O., Everson, R. C., & Neomagus, H. W. P. J. (2011). Fluidized-bed gasification of high-ash South African coals : An experimental and modelling study. *Proceedings of a conference of Fluidization*(November), 145–160.

Ergudenler, A., & Ghaly, A. E. (1993). Agglomeration of Alumina Sand in a Fluidized Bed Straw Gasifier at Elevated Temperatures. *Bioresource Technology*, *43*, 259–268.

Europe, I. E. (n.d.). *Final Guideline for Safe and Eco-friendly Biomass Gasification I . Preface* (Tech. Rep.).

Feng Duan, Lihui Zhang, Y. H. (2011). Dependence of bituminous coal gasification on pressure in a turbulent circulating fluidized bed. *Asi-Pacific Journal of Chemical Engineering*(October), 822–827.

Fu, Q., Deng, W., Saltsburg, H., & Flytzani-stephanopoulos, M. (2005). Activity and stability of low-content gold cerium oxide catalysts for the water gas shift reaction. *Applied Catalysis B: Environmental*, *56*, 57–68.

Ghaly, A. E., Ergudenler, A., & Ramakrishnan, V. V. (2015). Effect of Distributor Plate Configuration on Pressure Drop in a Bubbling Fluidized Bed Reactor. *Advances in Research*, *3*(3), 251–268.

Ghaly, A. E., & Macdonald, K. N. (2014). Mixing Patterns and Residence Time Determination in Bubbling Fluidized Bed System. *American Journal of Engineering and Applied Sciences,*, *5*(2), 170–183.

Gregory, R. W., Furimsky, E., & Mourits, F. M. (2006). *Coal Gasification.*

Harris, D. J., Roberts, D. G., & Henderson, D. G. (2006). Gasification behaviour of Australian coals at high temperature and pressure. *Fuel*, *85*, 134–142.

Hartman, M., Trnka, O., & Svoboda, K. (2000). Fluidization characteristics of dolomite and calcined dolomite particles. *Chemical Engineering Science*, *55*, 6269–6274.

Henderson, C., & Topper, J. M. (2005). Clean Coal Technologies and The Path to Zero Emissions. *Greenhouse Gas Control Technologies*, *II*, 1585–1591.

Inc., H. A., Princeton Energy Resources International, L., , , & Consulting, T. (2003). *Assessment of the Commercial Potential for Small Gasification Combined Cycle and Fuel Cell Systems Phase II* (Tech. Rep. No. March). U.S. Department of Energy Office of Fossil Energy Office of Coal and Power Systems.

Industrial Accident Prevention Association 2008. (2008). *Carbon Monoxide in the Workplace* (Tech. Rep.). IAPA.

Institute of Economic Affairs (IEA). (2015). *Situational Analysis of Energy Industry , Policy and Strategy for Kenya* (Tech. Rep.).

International Energy Agency(IEA). (2017). *Energy Technology Perspectives 2017 - Executive Summary* (Tech. Rep.).

Jiu Huang, K. G. S. Z. B. (2011). Removal and Conversion of Tar in Syngas

from Woody Biomass Gasification for Power Utilization Using Catalytic Hydrocracking. *Energies*, *4*, 1163–1177.

Jonathan M. Harris, B. R. (2017). Energy : The Great Transition. In *Environment and natural resource economics* (pp. 1–39).

Jorant, C. (2011). The implications of Fukushima. *Bulletin of the Atomic Scientists*, *67*(4), 14–17.

Karimipour, S., Gerspacher, R., Gupta, R., & Spiteri, R. J. (2013). Study of factors affecting syngas quality and their interactions in fluidized bed gasification of lignite coal. *Fuel*, *103*, 308–320.

Kenya National Bureau Of Statistics. (2017). *Statistical abst 2017 ct* (Tech. Rep.).

Kichonge, B., Mkilaha, I. S. N., & John, G. R. (2016). The Economics of Renewable Energy Sources into Electricity Generation in Tanzania. *Hindawi Publishing Corporation, Journal of Energy*, *3*(4), 1–13.

Krawczykowska, A., & Marciniak-kowalska, J. (2012). Problems of Water content in Lignites - Methods of its Reduction. *AGH Journal of Mining and Geoengineering*, *36*(4), 57–65.

Lars Waldheim, T. N. (2001). *Heating Value of Gases from Biomass Gasification* (Tech. Rep. No. May). IEA Bioenergy Agreement subcommittee on Thermal Gasification of Biomass.

Layton, B. E. (2008). A Comparison of Energy Densities of Prevalent Energy Sources in Units of Joules Per Cubic Meter of Joules Per Cubic Meter. *International Journal of Green Energy*, *5*(November 2008), 438–455.

Le Wu, Yu Qiao, H. Y. (2012). Experimental and numerical study of pulverized bituminous coal ignition characteristics in O 2 / N 2 and O 2 / CO 2 atmospheres. *Asia-Pacific Journal of Chemical Engineering*, *7*(April 2011), 195–200.

Lee, K., Brewer, E., Christiano, C., Meyo, F., Miguel, E., Podolsky, M., ... Wolfram, C. (2016). Electrification for "under Grid" households in Rural Kenya. *Development Engineering*, *1*, 26–35.

Li, F., & Fan, L.-s. (2008). Clean coal conversion processes progress and challenges. *Energy & Environ. Sci*, *1*, 248–267.

Liu, H., Ni, W., Li, Z., & Ma, L. (2008). Strategic thinking on IGCC development in China. *Energy policy*, *36*, 1–11.

Liu, H., Zhu, H., Yan, L., Huang, Y., Kato, S., & Kojima, T. (2011). Gasification reactivity of char with CO 2 at elevated temperatures : the effect of heating rate during pyrolysis. *Asi-Pacific Journal of Chemical Engineering*, *6*(July

2010), 905–911.

Liu, Q., Shi, M., & Jiang, K. (2009). New power generation technology options under the greenhouse gases mitigation scenario in China. *Energy policy*, *37*, 2440–2449.

Lyman, R. (2016). Why Renewable Energy Cannot Replace Fossil Fuels By 2050 a Reality Check. *Friends of Science*(May), 44.

Mamoru Kaiho and Osamu Yamadablished (National Institute of Advanced Industrial Science and Technology Japan). (n.d.). Stoichiometric Approach to the Analysis of Coal Gasification Process. In D. A. Innocenti (Ed.), *Stoichiometry and materials science - when numbers matter* (pp. 415–436). intech: InTech.

Martelli, E., Kreutz, T., & Consonni, S. (2009). Comparison of coal IGCC with and without CO 2 capture and storage : Shell gasification with standard vs . partial water quench. *Energy Procedia*, *1*(1), 607–614.

Miller, B. G., & Tillman, D. A. (2008). Coal Characteristics. *Combustion Engineering Issues for Solid Fuel Systems*(October), 33–81.

Ministry of Energy Republic of Kenya. (2015). *National Energy and Petroleum Policy* (Tech. Rep.).

Na, J. I., Park, S. J., Kim, Y. K., Lee, J. G., & Kim, J. H. (2003). Characteristics of oxygen-blown gasification for combustible waste in a fixed-bed gasifier. *Applied energy*, *75*, 275–285.

Nor Fadzilah Othman, Mohd Hariffin Bosrooh, K. A. M. (2007). Partial Gasification of Different Types of Coals in a Fluidised Bed Gasifier. *Jurna Mekanikal*(23), 40–49.

Nowak, W. (2003). Clean coal fluidized-bed technology in Poland. *Applied Energy 74*, *74*, 405–413.

Ocampo, A., Arenas, E., Chenjne, F., & Espinel, J. (2003). An Experimental Study on Gasification of Chicken Litter. *Fuel*, *82*(1), 161164.

Octave Levenspiel, D. K. (1991). *Fluidization Engineering* (2nd ed.).

Philip R. Bevington, D. K. R. (2003). *Bevington_opt.pdf* (THIRD ed.). Kent A. Peterson.

Phillips, J. (2006). Different types of gasifiers and their integration with gas turbines. *The Gas Turbine Handbook*, 67–77.

Professor Prabir Basu. (2006). *Combustion and Gasification In Fluidized Beds*. Taylor & Francis Group, LLC.

Ramirez, J., Martinez, J., & Petro, S. (2007). Basic Design of a Fluidized Bed gasifier for Rice Husk on a Pilot Scale. *Latin American Applied Research*,

37, 299–306.

Reclamation, W. P. C. f. A. M. (n.d.). *How do I get rid of my waste coal pile ? Burning Waste Coal in CFB Power Plants* (No. 724).

Sara Mcallister, Jyh-Yuan Chen, A. C. F.-P. (n.d.). *Fundamentals of Combustion Processes*. Springer.

Seo, H.-k., Park, S., Lee, J., Kim, M., Chung, S.-w., Chung, J.-h., & Kim, K. (2011). Effects of operating factors in the coal gasification reaction. *Korean J. Chem. Eng*, *28*(9), 1851–1858. doi: 10.1007/s11814-011-0039-z

Shadle, L. J., Breault, R. W., & Bennet, J. (2017). *Gasification Technology* (No. January 2012). doi: 10.1007/978-1-4419-7991-9

Shakorfow, A. M. (2016). Operating and Performance Gasification Process Parameters. *International Journal of Science and Research*, *5*(6), 1768–1775.

Staff, G. C., & Project, E. (2006). *Global Climate & Energy Project Technical Assessment Report A Technical Assessment of Coal Utilization and Research Trends GCEP Energy Assessment Analysis* (Tech. Rep.). Stanford University.

Suleiman, Y., Ibrahim, H., Anyakora, N. V., Mohammed, F., Abubakar, A., Aderemi, B. O., & Okonkwo, P. C. (2013). Design and Fabrication of Fluidized Bed Reactor. *International Journal of Engineering and Computer Science*, *2*(5), 1595–1605.

Tasma, D., & Uzunanu, K. (2007). "The effect of excess air ratio on syngas produced by gasification of agricultural residues briquettes". *Carbon*, *29*(24.85), 22–60.

Tremel, A., Haselsteiner, T., Kunze, C., & Spliethoff, H. (2012). Experimental investigation of high temperature and high pressure coal gasification. *Applied Energy*, *92*, 279–285.

Umeki, K., Yamamoto, K., Namioka, T., & Yoshikawa, K. (2010). High temperature steam-only gasification of woody biomass. *Applied Energy*, *87*(3), 791–798.

Wong, L., & David de Jager and Pieter van Breevoort April. (2016). *The incompatibility of high-efficient coal technology with 2 C scenarios* (Tech. Rep.).

Wormsbecker Michael, Todd s. Pugsley, H. T. (2007). The Influence of Distributor Design on Fluidized Bed Dryer Hydrodynamics Michael..

Xiaojiang W., Zhongxiao Z.,Guilin P., Nobusuke K., Shigekastu M., Y. I. (2010). Experimental study on gasification characteristics and slagging behavior of Chinese typical high ash fusion temperature coal in lab scale downflow

gasifier. *Asia-Pacific Journal of Chemical Engineering*, *5*(May 2009), 427–434.

Zhang, X. (2016). *Emission standards and control of PM 2 . 5 from coal-fired power plant* (Tech. Rep. No. July). IEA Clean Coal Centre.

Zhao, L., Xiao, Y., Sims, K., Wang, B., & Xu, X. (2008). Technical , environmental , and economic assessment of deploying advanced coal power technologies in the Chinese context. *Energy policy*, *36*(November 2006), 2709–2718.

Zhu, Q. (2015). *High temperature syngas coolers* (Tech. Rep. No. September). IEA Clean Coal Centre.

APPENDIX I

Gasifier Design Calculations

A.1 Coal Molecular Formula

The atomic weights of the specific components in the coal used are as shown in Table A.1 below.

Table A.1: Specific components in coal and their atomic weights

Constituents	**% by weight (kg)**	**Atomic wt (kg/kmol)**
Carbon	65.44	12
Hydrogen	4.6	2
Oxygen	7.82	32
Nitrogen	1.07	28
Sulphur	3.61	32
H_2O	4.09	18

Determination of moles of each of the fuel constituent used:

$$\begin{aligned} carbon &= \frac{65.44\ kg}{12\ kg/mole} = 5.453\ moles \\ hydrogen &= \frac{4.60\ kg}{1\ kg/mole} = 4.60\ moles \\ oxygen &= \frac{7.82\ kg}{16\ kg/mole} = 0.489\ moles \end{aligned}$$

C, H, and O were used to form chemical equation as $C_{5.453}H_{4.60}O_{0.489}$ which was normalized as shown below:

$$\begin{pmatrix} 5.453\ C \\ 4.60\ H \\ 0.489\ O \end{pmatrix} = 5.453 \begin{pmatrix} C \\ 0.844\ H \\ 0.090\ O \end{pmatrix}$$

A.2 Stoichiometric Air Required

At stoichiometric condition, all the carbon in the fuel will be converted to carbon dioxide and water. The balanced chemical equation was obtained as shown;

$$C_{5.453}H_{4.6}O_{0.489} + 6.3585O_2 + \rightarrow 5.453CO_2 + 2.30H_2O \tag{5.1}$$

This equation can be re-written as;

$$CH_{0.844}O_{0.090} + 1.166O_2 \rightarrow CO_2 + 0.422H_2O \tag{5.2}$$

The rate of air supply for combustion of 5kg/h in g/s is given by

$$\dot{m}_f = \frac{5000}{3600} = 1.389 g/s \tag{5.3}$$

From the ultimate analysis of coal the carbon percentage was obtained as 65.44 % so the carbon mass flow rate $\dot{m}_c$ was given by;

$$\dot{m}_c = 0.6544 \times \dot{m}_f = 0.9090 g/s \tag{5.4}$$

Fuel carbon flow rate $\dot{\eta}_c$ was given by

$$\dot{\eta}_c = \frac{\dot{m}_c}{M_c} = \frac{0.9090}{12} = 0.07575 moles/s \tag{5.5}$$

Oxygen molar flow rate $\dot{\eta}_O$ was determined as shown

$$\dot{\eta}_O = \dot{\eta}_c \times SCO_2 = 0.07575 \times (1.166 + 0.090) = 0.0951 moles/s \tag{5.6}$$

where SCO_2 is the amount of oxygen required for stoichiometric combustion to take place. Oxygen volume flow rate at room temperature and pressure $\dot{V}_O$ was given as

$$\dot{V}_O = 24L/mole \times \dot{\eta}_O = 24L/mole \times 0.0951 = 2.2824 L/s \tag{5.7}$$

24L/mole is the capacity of atmospheric air at standard conditions. Atmospheric air volume flow rate $\dot{V}_a$ was therefore estimated as follows;

$$\dot{V}_a = \frac{V_O}{0.21} = \frac{2.2824}{0.21} = 10.8686 L/s = 0.0108 m^3/s \tag{5.8}$$

A.3 Equivalence Ratio

The equivalence ratio was determined from the stoichiometric air fuel ratio and the actual air fuel ratio during gasification. From the stoichiometric equation of coal combustion and by using equation 5.9 the air fuel ratio AFR_s was obtained as

$$AFR_s = \frac{m_a}{m_f} \tag{5.9}$$

$$AFR_s = \frac{6.3585(4.76)[Kmol]29Kg/Kmol}{1[Kmol]\,(5.453(12) + 4.6 + 0.489(16))} = 11.274 \tag{5.10}$$

The gasification equivalence ratio (ϕ) was calculated using Equation 5.11 :

$$\phi = \frac{m_a/m_f}{m_{as}/m_f} \tag{5.11}$$

where m_a and m_asas are mass of air and mass of stoichiometric air while m_f is the mass of fuel. Equation **??** then simplifies to equation 5.12 below

$$\phi = \frac{m_a}{m_{as}} \tag{5.12}$$

Using equation 5.12 the equivalence ratios of the gasification process at different flow rates was calculated and tabulated in Table A.2;

Table A.2: Equivalence Ratios at different Flow Rates

Air Flow Rate (m^3/min)	0.5	1.0	1.5	2.0
Equivalence ratio(ϕ)	0.282	0.283	0.345	0.359
Mass of air (Kg)	2.541	2.553	3.109	3.234
Mass of syngas (Kg/Kg of Coal)	3.541	3.553	4.109	4.234

The mass of syngas (m_{sy}) obtained during gasification was obtained by summing up the mass of air (M_a) to the mass of coal (M_C) consumed per hour as shown in Equation 5.13 (CENCERE(Centre for Clean Energy Research and Education), n.d.).

$$M_{sy} = M_C + M_a \tag{5.13}$$

APPENDIX II

Preliminary Work

B.1 Air Blower Calibration

The gasifying air was supplied by a Black & Decker blower with variable flow rates; from level 1 to level 6. The levels could not be quantified as only the maximum flow rate of 3.5m$^3/min$ was provided on the manual. To obtain the flow rates at the specific levels calibration was necessary. This was done using an air flow bench as discussed in Section 3.4 of the Experimental Design and Methodology. the results of the calibration are presented in Table B.1;

Flow Level	Flow Rate (m^3/min)
1	1.04
2	1.48
3	2.02
4	2.49
5	2.98
6	3.50

Table B.1: Flow Rates of Blower at Different levels

APPENDIX III

Results Data

C.1 Syngas Composition

The results of the composition test are tabulated in Table C.1

Table C.1: Syngas Composition

Air flow rate (m^3/min)	CO(%)	H_2(%)	CO_2(%)	CH_4
1.0	20.61	9.6	15.17	4.62
1.5	22.92	7.16	14.61	3.92
2.0	18.29	6.94	15.57	3.17
2.5	17.78	5.69	16.23	2.85

C.2 Reactor Temperatures

The average reactor temperatures at different air flow rates are presented in Table C.2

Table C.2: Reactor Temperatures at Different Air Flow Rates

Air Flow Rate (m^3/min)	1.0	1.5	2.0	2.5
Reactor Temperature(K)	1173	1130	1134	1146
Reactor Temperature(^{o}C)	850	857	861	873

C.3 Higher Heating Value of syngas

Using the HHV of constituent gases of the syngas the HHV of the syngas was calculated and the results are as shown in Table C.3.

Table C.3: Syngas Calorific Value Estimated Results

Air Flow Rate (m^3/min)	1.0	1.5	2.0	2.5
Calorific Value (MJ/Nm^3)	5.667	5.369	4.457	4.106

C.4 Effect of Air Flow Rate on NO_x and SO_2 Emissions

The emission concentration in the syngas are presented in Table C.4

Table C.4: Emission Results

Air Flow Rate (m^3/min)	1.0	1.5	2.0	2.5
NO_x (ppm)	60	79.5	103	110
SO_2 (ppm)	215	302	314	333

C.5 Effect of Air Flow Rate Syngas outlet Temperatures

The temperature of the syngas at the outlet of the gasifier is shown in TableC.5

Table C.5: Temperatures of Syngas at the outlet of the free board Section

Air Flow Rate (m^3/min)	1.0	1.5	2.0	2.5
Outlet Syngas Temperatures (^oC)	375.00	541.65	577.60	545.40